

Chapter 2

Fundamentals of Planar Metamaterials and Subwavelength Resonators

Electromagnetic metamaterials have been a subject of huge research worldwide in the electromagnetic and microwave communities since the first so-called left-handed structure was experimentally conceived in 2000. These efforts have been primarily motivated by the exotic (unusual) electromagnetic properties that these artificial media may feature, such as backward wave propagation. Meanwhile, electrically small resonators (ESRs) based on split rings, which are typical key building blocks to the synthesis of metamaterials, have been investigated broadly as well. The research activity on these resonant particles has been focused not only on the implementation of metamaterials, but also on the design of RF/microwave circuits and components. Thus, novel ideas have emerged in the microwave community to envisage devices inspired by metamaterial concepts with high performance, small size and/or new functionalities. In this regard, in the present thesis these metamaterial-based particles are not utilized to construct metamaterial structures, but to design innovative RF/microwave devices. Nonetheless, a brief introduction to metamaterials is provided for a historical standpoint and to make the thesis more complete, although reporting the current state-of-the-art is beyond the scope of this thesis.

This chapter is devoted to planar metamaterials and electrically small split-ring resonators, mainly from a circuit approach perspective. It should be mentioned that a significant part of the intensive work in such topics has been published in textbooks by several pioneering research groups in the last decade [1–6]. Section 2.1 provides a brief description of the fundamental properties of metamaterials as well as a historical overview. In Sect. 2.2, the different approaches of transmission-line metamaterials are introduced, which are of particular interest to the microwave community. Specifically, the main focus is aimed at the so-called resonant-type approach in planar technology where subwavelength resonators are used for its synthesis. Inside this category, structures with stopband characteristics will receive the most attention. Next, Sect. 2.3 is aimed at describing subwavelength resonators that are used throughout this thesis, with special emphasis on the properties derived from

symmetry assumptions. Finally, Sect. 2.4 is addressed to waves induced in chains of coupled resonators, namely, electro-inductive and magneto-inductive waves.

2.1 Electromagnetic Metamaterials

Electromagnetic metamaterials may be broadly defined as *artificial* (man-made) *effectively homogeneous structures* (usually made up of an arrangement of metals and dielectrics) *with unusual properties not readily available in nature* [1].¹ Certainly, the prefix *meta* means *beyond* or *after* in Greek, suggesting that the medium possesses properties that transcend those available in natural materials, this being the most relevant characteristic of metamaterials.²

A medium is regarded to be effectively (on average) homogeneous (uniform) if its unit-cell dimension is much smaller than the guided wavelength. This homogenization (averaging) procedure is the key to considering the structure electromagnetically homogeneous along the direction of propagation. Consequently, a metamaterial behaves as a real material in the sense that the macroscopic (in a piece of matter) response to an electromagnetic field can be characterized by effective macroscopic constitutive parameters, namely, the permittivity ϵ and the permeability μ [1, 2]. Indeed, this approach is a direct translation of the characterization of natural media, which are made of atoms and molecules with dimensions many orders of magnitude smaller than the wavelength; the original objective in defining a permittivity and a permeability was to present an homogeneous view of the electromagnetic properties of a discrete natural medium. Analogously, metamaterials are usually synthesized by embedding a periodic³ array of artificial small inclusions (man-made atoms and molecules) at a sufficiently electrically small mutual distance in a specified host medium [2]. Therefore, the design parameters in the synthesis process of a metamaterial (such as the shape, arrangement or alignment of the inclusions) provide a large collection of independent parameters (or freedom degrees) in order to engineer an artificial material with a specific controllable electromagnetic response different from that obtained by its constitutive materials [2]. In summary, the macroscopic view of metamaterials consists of replacing an artificial structurally inhomogeneous structure with an effectively homogeneous medium characterized by effective constitutive parameters.

¹Since the international scientific community has not achieved a consensus in the definition of electromagnetic metamaterials [6], other artificial inhomogeneous structures with controllable electromagnetic properties (e.g. electromagnetic bandgaps—EBGs—which are based on the Bragg regime) are also sometimes regarded as metamaterials [2].

²The subject has been known for a long time as artificial dielectrics, composite materials, or microstructured materials. The aim has always been to reproduce physical responses of known materials or to obtain some desirable responses not readily available in nature.

³Periodicity is not fundamental, but eases the design.

2.1.1 Material Classification

Since the response of a medium to an electromagnetic field is determined by its properties (ϵ and μ),⁴ this allows for the classification of a medium depending on the sign of the constitutive parameters, as illustrated in Fig. 2.1 [1, 2]. Media with both permittivity and permeability greater than zero are known as *double-positive* (DPS) media. A medium with either permittivity or permeability less than zero is designated as *epsilon-negative* (ENG) medium or *mu-negative* (MNG) medium, respectively, or alternatively *single-negative* (SNG) medium in both scenarios. More interestingly, media with negative permittivity and permeability are called *double-negative* (DNG) media, following the preceding nomenclature. Nevertheless, several other terminologies have been suggested, such as *left-handed* (LH), *backward-wave* (BW), and *negative-refractive index* (NRI) media [1, 2].⁵ While natural DPS and SNG media are known to exist (see Fig. 2.1), a DNG medium has not been found in nature to date [1, 2], and for this reason the most popular metamaterials in the considered classification belong to this category [1]. As will be explained in Sect. 2.1.2, DNG media may be synthesized artificially by pairs of elements, in which an array of one of the elements produces a negative effective permittivity and an array of the other element induces a negative effective permeability.

As is well known, the propagation of electromagnetic waves through a medium at the macroscopic level is governed by Maxwell's equations, and such a propagation depends on the constitutive parameters as follows. When either permittivity or permeability is negative, the medium supports only non-propagating evanescent modes (the medium is opaque to signal transmission). Consequently, there cannot be energy transfer through the medium because the incident electromagnetic waves suffer reactive attenuation (reflection, but not dissipation⁶) and decay exponentially in amplitude away from the source [4, 7]. By contrast, when permittivity and permeability are both either positive or negative, wave propagation inside a medium is possible (the medium is said to be transparent).

2.1.2 Left-Handed Media

Left-handedness expresses the fact that the propagation of plane waves is described by the electric field \mathbf{E} , the magnetic field \mathbf{H} , and the wave vector or propagation constant \mathbf{k} building a left-handed triplet, in contrast to conventional materials (with positive constitutive parameters) where this triplet is right-handed (see Fig. 2.2). However, \mathbf{E} , \mathbf{H} , and the Poynting vector \mathbf{S} maintain a right-handed relationship. As a consequence, the phase velocity (parallel to the direction of phase propagation or

⁴If losses are absent, as is assumed throughout this chapter, ϵ and μ are real numbers.

⁵The term NRI describes the particularity that the index of refraction in these media is negative, while the terminologies LH and BW will be addressed shortly.

⁶Recall that losses are precluded in the whole chapter.

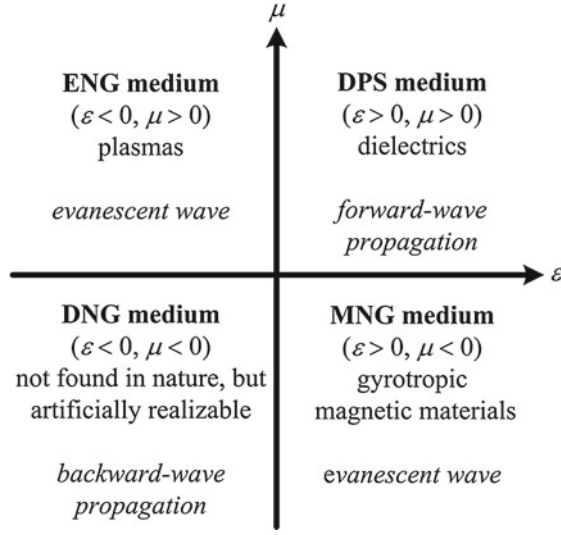


Fig. 2.1 Material classification according to the sign of permittivity-permeability

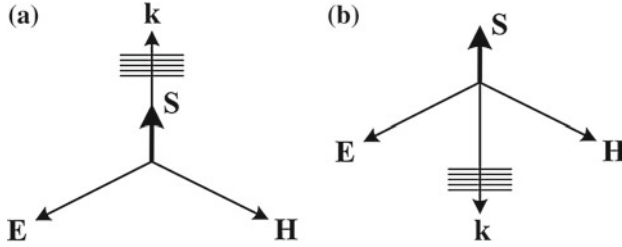


Fig. 2.2 Orientation of the electric field **E**, magnetic field **H**, propagation constant **k**, and Poynting vector **S** for a transverse electromagnetic (TEM) plane wave in an orthogonal system of vectors, as prescribed by Maxwell's equations. **a** Right-handed medium. **b** Left-handed medium

propagation constant) given by⁷

$$v_p = \frac{\omega}{\beta}, \quad (2.1)$$

and the group velocity (parallel to the direction of power flow or Poynting vector) defined as

$$v_g = \frac{d\omega}{d\beta}, \quad (2.2)$$

travel in opposite directions, a physical phenomenon that is called *backward-wave* propagation.

⁷In the literature the propagation constant is represented by k or β [8]. Hereafter the symbol β will be used since it is the usual convention in microwave engineering.

Therefore, LH media are characterized by the propagation of waves exhibiting anti-parallel⁸ phase and group velocities, contrary to the case of wave propagation in conventional media that is known to be *forward* [1–4].⁹ As a result, it follows that, since energy transfer is always outward from the source, the direction of propagation of the wavefronts in a LH medium is inward to the source. In consequence, the phase of a backward wave increases in the direction of group velocity (phase advance), in contrast to conventional materials which introduces a negative phase (phase lag). It is also worth mentioning that backward-wave propagation has implications in well known physical effects related to electromagnetic wave propagation, such as the reversal of Snell's law, Doppler effect, and Cherenkov radiation [1, 3].

The history of metamaterials may be considered to start in 1967 with the seminal work by Veselago [11], who examined the feasibility of media characterized by simultaneously negative permittivity and permeability. He concluded that such media are allowed by Maxwell's equations, establishing their fundamental properties and predicting some unusual electromagnetic phenomena, such as backward-wave propagation and left-handedness. Accordingly, he labeled conventional materials as RH media, and media with negative constitutive parameters as LH media.

Although Veselago may be considered the father of left-handed media [1], more than 3 decades elapsed until the first LH material was conceived and experimentally demonstrated by Smith et al. in 2000 [12]. This metamaterial was a composite structure of conducting wires and split-ring resonators (SRRs) [13], as shown in Fig. 2.3a. The effective permeability of an array of SRRs becomes negative in a narrow band above their resonance frequency, and a stopband response arises in the vicinity of that frequency. Conversely, an array of parallel thin metallic wires produces an effectively negative permittivity below a cutoff frequency,¹⁰ exhibiting a highpass behavior. Thereby a proper combination of SRRs and wires (i.e. achieving a frequency region with simultaneously negative constitutive parameters), the stopband near the resonance of the SRRs switches to a passband with a LH signature (see Fig. 2.3b). Although this metamaterial is a bulk construction, since left-handed behavior occurs for a specific polarization and direction of propagation of the incident electromagnetic field, this structure can be viewed as a one-dimensional metamaterial. It should be noted that a LH medium made of natural media may also be possible. Unfortunately, the negative value of the constitutive parameters occurs at different frequency bands, preventing simultaneously negative permittivity and permeability [3].

⁸Anti-parallel vectors are collinear vectors (lying in the same line) with opposite directions.

⁹Backward-wave propagation has been known for decades. For instance, periodic structures support an infinite number of positive (forward) and negative (backward) space harmonics in addition to the fundamental space harmonic [7, 9]. The novelty of LH materials is that they are effectively homogeneous structures operating in a backward fundamental space harmonic [1, 2]. Forward/backward waves should not be confused with forward-/backward-traveling waves which are simply forward waves traveling in the positive/negative direction of propagation [10]. The latter are also known as positive- and negative-going waves [1].

¹⁰This cutoff frequency is usually called plasma frequency in analogy to the permittivity function of a plasma.

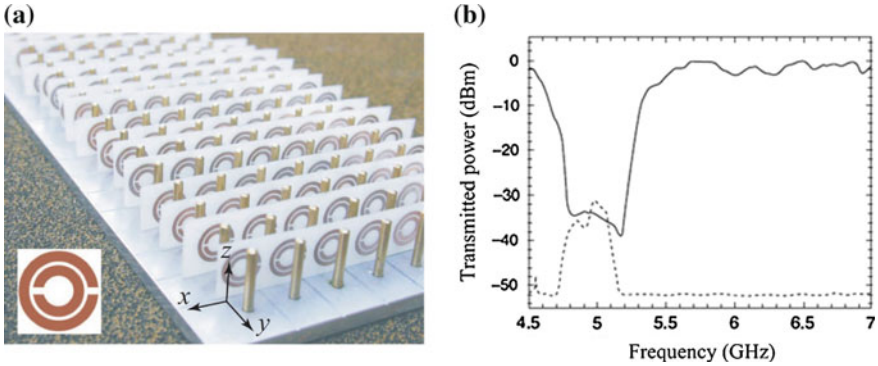


Fig. 2.3 First artificially synthesized LH structure. **a** Photograph reprinted with permission from [1]. **b** Transmitted power (x -axis orientation) when only SRRs are considered (*solid line*) and when wires and SRRs are present (*dashed line*). The incident electric field is parallel to the wires (z -axis), while the incident magnetic field is polarized along the axis of the rings (y -axis)

2.2 Transmission-Line Metamaterials

Transmission-line metamaterials (or *metamaterial transmission lines*)¹¹ are *artificial transmission lines* [6] that consist of a host (conventional) transmission line¹² loaded with reactive elements, the latter providing higher design flexibility in comparison to conventional lines [3, 4, 6]. Specifically, one-dimensional (1D) transmission-line metamaterials are effectively homogeneous structures whose electromagnetic characteristics can be controlled or engineered to some extent through a specific direction of propagation (this definition is, however, revised in Sect. 2.2.5).

2.2.1 Application of the Transmission-Line Theory to Metamaterials

Soon after the first experimental demonstration of left-handedness, several pioneering groups focused their research efforts on developing a transmission-line approach (non-resonant) of metamaterials exhibiting backward-wave propagation [14–16].

The reported approach originates from the fact that Maxwell's equations with plane-wave propagation in homogeneous and isotropic media have an identical form to the equations describing TEM propagation on a transmission line derived from

¹¹In this thesis *transmission-line metamaterials* and *metamaterial transmission lines* are synonyms because this book deals with one-dimensional (1D) structures. When the same concept is extended to 2D and 3D dimensions, the structures are referred to as transmission-line metamaterials (i.e. metamaterial transmission lines apply only to 1D structures) [6].

¹²Note that host transmission lines are commonly implemented on an ordinary dielectric substrate whose permittivity is different from the effective permittivity of the metamaterial.

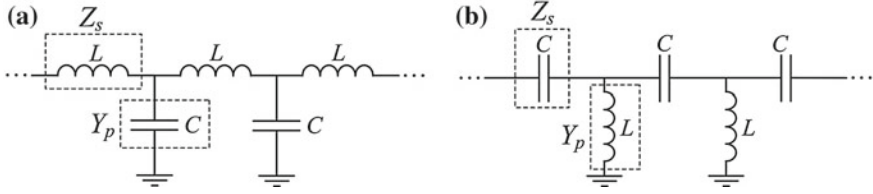


Fig. 2.4 Equivalent circuit model of a transmission line. **a** Conventional or RH transmission line. **b** Dual or LH transmission line

circuit theory, known as the telegrapher equations. Hence, such an analogy allows the series and shunt elements of the well-known ladder circuit model of a transmission line to be related to the constitutive parameters of a medium (exhibiting the same propagation characteristics) by mapping the telegrapher equations to Maxwell's equations. The resulting relationships are [1–4]

$$Z'_s = Z_s/l = j\omega\mu, \quad (2.3a)$$

$$Y'_p = Y_p/l = j\omega\epsilon, \quad (2.3b)$$

where Z'_s and Y'_p are the (distributed) per-unit-length series impedance (Ω/m) and shunt admittance (S/m), respectively, Z_s and Y_p are the per-unit-cell series impedance (Ω) and shunt admittance (S), respectively, and l is the unit cell length (the period).

Accordingly, in conventional RH media, the mapping yields

$$\mu = L' = L/l, \quad (2.4a)$$

$$\epsilon = C' = C/l, \quad (2.4b)$$

where L' and C' are the per-unit-length series inductance (H/m) and shunt capacitance (F/m), respectively, while L and C represent the per-unit-cell series inductance (H) and shunt capacitance (F), respectively. The resulting well-known equivalent circuit is shown schematically in Fig. 2.4a, whose propagation is forward with a propagation constant and a characteristic impedance given by

$$\beta_R = \omega\sqrt{L'C'}, \quad (2.5a)$$

$$Z_{cR} = \sqrt{\frac{L'}{C'}}, \quad (2.5b)$$

respectively. In the transmission-line approach of metamaterials the previous well-established analogy has been extended to the other (exotic) combinations of the constitutive parameters depending on their sign. Thus, for a LH medium, the series inductance and the shunt capacitance should become negative according to (2.4). Since from an impedance perspective a negative inductance/capacitance may be interpreted as a positive capacitance/inductance [2], a ladder network as the one

depicted in Fig. 2.4b with series-connected capacitors and shunt-connected inductors supports the propagation of backward waves. Such a network is called the *dual*¹³ of the equivalent circuit of a RH transmission line. The mapping in this dual network yields

$$\mu = -\frac{1}{\omega^2 C'} = -\frac{1}{\omega^2 C l}, \quad (2.6a)$$

$$\epsilon = -\frac{1}{\omega^2 L'} = -\frac{1}{\omega^2 L l}, \quad (2.6b)$$

where C' and L' are now the time-unit-length¹⁴ series capacitance ($\text{F} \cdot \text{m}$) and shunt inductance ($\text{H} \cdot \text{m}$), respectively, while C and L stand for the per-unit-cell series capacitance (F) and shunt inductance (H), respectively. The corresponding propagation constant and characteristic impedance become

$$\beta_L = -1/\omega \sqrt{L' C'}, \quad (2.7a)$$

$$Z_{cL} = \sqrt{\frac{L'}{C'}}, \quad (2.7b)$$

respectively. Contrarily to a dispersionless RH line, a LH transmission line is intrinsically dispersive by nature because its propagation constant is not a linear function of frequency. It should also be emphasized that the mapping given in (2.3) is valid only in the long wavelength regime, where the period is much smaller than the guided wavelength

$$\lambda_g = \frac{2\pi}{|\beta|}, \quad (2.8)$$

which is defined only in the passbands [1]. Only under this circumstance the definition of effective constitutive parameters is fully feasible and a ladder circuit may describe a RH or LH transmission line.

Figure 2.5 summarizes the generalization [2] of the aforementioned transmission-line approach of metamaterials by means of unit-cell equivalent T-circuit models. Besides the RH (or DPS) and LH (or DNG) transmission lines, the equivalent circuits of SNG transmission lines are also indicated. It should be noted that waves cannot propagate in either ENG or MNG transmission lines because their models are exclusively made up of inductors or capacitors. As wavelength cannot be defined, these models should be interpreted conceptually. To sum up, the transmission-line theory in metamaterials links field to circuit quantities, offering an alternative interesting physical interpretation leading to the same functional results.

¹³Duality is defined here in terms of complementary response (e.g. the dual of a lowpass filter is a highpass filter) so that the series/shunt impedance of a network is proportional to the series/shunt admittance of the other network.

¹⁴This ensures properly defined units in Z'_s (Ω/m) and Y'_p (S/m).

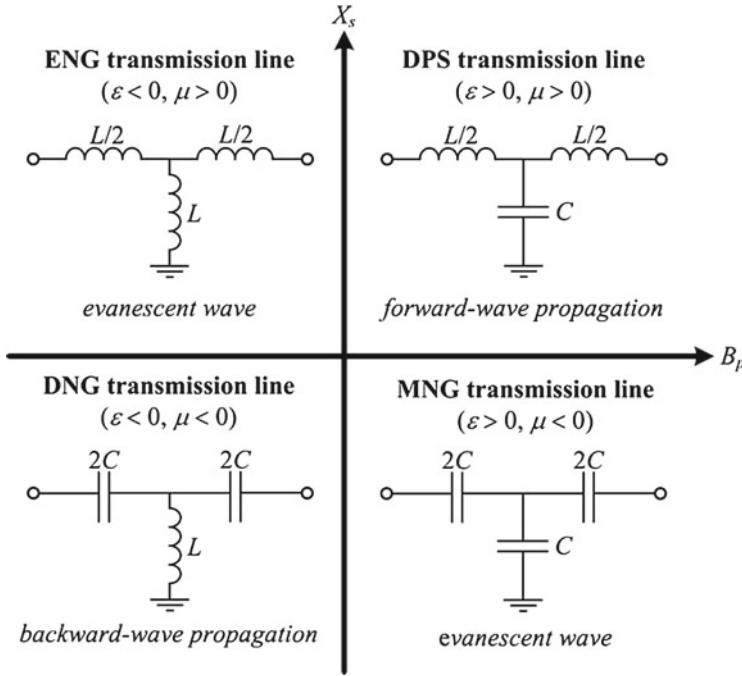


Fig. 2.5 Unit-cell equivalent T-circuit models of transmission lines according to the sign of the series reactance, X_s ($Z_s = jX_s$), and shunt susceptance, B_p , ($Y_p = jB_p$). The validity of these models is restricted to the long wavelength regime. Since wavelength cannot be defined if propagation is forbidden, as occurs in ENG and MNG transmission lines, these models are conceptual interpretations

2.2.2 Composite Right-/Left-Handed (CRLH) Transmission Lines

From a practical point of view, a purely left-handed (PLH) transmission line as that depicted in Fig. 2.4b cannot be implemented. A necessary host transmission line introduces inevitably parasitic elements, as illustrated in Fig. 2.6 [1–4]. Since these elements cannot be neglected in general and induce wave propagation of forward nature, practical realizations of left-handed transmission lines exhibit left- or right-handed propagation, depending on the frequency interval. For this reason, such lines are termed composite right-/left-handed (CRLH) transmission lines [17], and they constitute the most general transmission-line metamaterial [1]. Indeed, as will be shown shortly, a CRLH line is able to behave as a DPS, DNG, or ENG/MNG transmission line within particular frequency ranges.

Instead of describing the transmission characteristics of CRLH lines obtaining their effective constitutive parameters by (2.3), Fig. 2.7 shows the typical dispersion

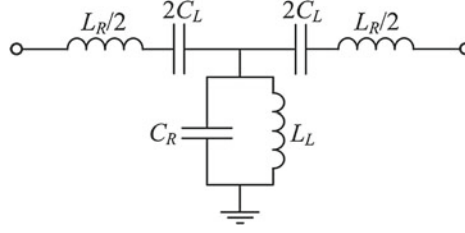


Fig. 2.6 Unit-cell equivalent T-circuit of a composite right-/left-handed (CRLH) transmission line; the subscripts L and R stand for the corresponding LH and RH elements, respectively

diagram¹⁵ of a CRLH line, which indicates the variation of the propagation constant with frequency. Hence, the dispersion diagram reveals the passbands/stopbands as well as the nature (RH or LH) of the passbands since the phase and group velocities can be easily inferred from (2.1) and (2.2), respectively.¹⁶ As can be seen, if $\omega < \min(\omega_s, \omega_p)$, $v_p < 0$ and $v_g > 0$ have opposite signs, meaning that propagation is backward. Conversely, when $\omega > \max(\omega_s, \omega_p)$, $v_p > 0$ and $v_g > 0$ exhibit the

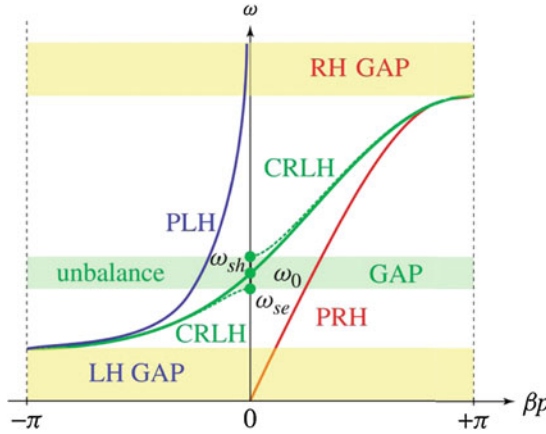


Fig. 2.7 Typical dispersion diagram for an unbalanced/balanced CRLH transmission line. The period is $p = l$, while the series and shunt resonances are indicated as $\omega_{se} = \omega_s = 1/\sqrt{L_R C_L}$ and $\omega_{sh} = \omega_p = 1/\sqrt{L_L C_R}$, respectively. The case with $\omega_s < \omega_p$ is illustrated, although $\omega_s > \omega_p$ is also possible. The curves for a purely RH (PRH) line ($L_L = C_L \rightarrow \infty$) and for a purely LH (PLH) line ($L_R = C_R = 0$) described by (2.5a) and (2.7a), respectively, are also shown. Reprinted with permission from [2]

¹⁵The calculation procedure of the dispersion relation of a periodic structure composed of a cascade of two-port unit-cell circuits is well-known (Appendix A).

¹⁶The phase velocity is the slope of the line segment from the origin of the dispersion curve $\omega(\beta)$ to a point in the curve, whereas the group velocity is the slope of the tangent to the dispersion curve at a point.

same sign, indicating that wave propagation is of forward nature.¹⁷ The frequency at the transition from a passband to a stopband ($\beta l = 0$ or $\pm\pi$) is often called cutoff frequency [10], being the group velocity equal to zero. There are some stopbands (or bandgaps) in the CRLH line, characterized by evanescent waves caused by reflections. When $\omega \rightarrow 0$ there is a stopband due to the highpass nature of the LH elements, whereas when $\omega \rightarrow \infty$ a stopband arises because of the lowpass behavior of the RH components. It is thus apparent that the transmission characteristics of a CRLH line at low and high frequencies tend to behave as purely LH and RH transmission lines, respectively (this is due to periodicity, since a RH transmission line exhibits an all-pass response at all frequencies). In addition, in the general case when the series resonance, ω_s , does not coincide with the shunt resonance, ω_p , a stopband appears between these frequencies, and the line is known to be *unbalanced*. By contrast, in the case that these frequencies are equal, $\omega_s = \omega_p = \omega_0$, there is a continuous transition between the left- and right-handed bands,¹⁸ and the CRLH line is said to be *balanced*¹⁹ [1–3].

The guided wavelength,²⁰ given by (2.8), can also be readily derived from the dispersion curve. As mentioned in Sect. 2.1, an effectively homogeneous structure is defined as that whose unit cell size l is much smaller than λ_g . The effective-homogeneity condition is usually $l < \lambda_g/4$ [1], which in terms of the electrical length becomes $|\beta l| < \pi/2$. Since in the unbalanced configuration the structure is effectively homogeneous at the edges of the bandgap that ranges from ω_s to ω_p , this stopband in terms of the constitutive parameters is said to be due to either $\epsilon < 0$ (if $\omega_s < \omega_p$) or $\mu < 0$ ($\omega_s > \omega_p$) [1]. By contrast, the stopbands at low and high frequencies are not near the long wavelength regime. Therefore, at these frequencies, effective constitutive parameters cannot be rigorously defined and the circuit model of Fig. 2.6 is no longer valid to represent an effectively homogeneous CRLH transmission-line metamaterial. In order to model correctly RH/LH (or CRLH) transmission lines at higher/lower frequencies, one needs to reduce the period, and accordingly to reduce/increase the per-section inductance and capacitance given in (2.4)/(2.6), so that operation in the long wavelength regime holds. In other words, the circuit models of RH/LH/CRLH transmission lines mimic transmission lines only in their passbands where homogeneity is satisfied. Note that the circuit model of a CRLH transmission line is the same as that of a bandpass filter, and the circuits of RH and LH lines are lowpass and highpass filters, respectively [18]. Classical filters, however, are characterized at all frequencies (from $\omega = 0$ to $\omega \rightarrow \infty$). Therefore, as a fundamental property, filters exhibit both passband and stopband characteristics according to the filter type.

¹⁷Alternatively, when $|\beta|$ increases with frequency, v_p and v_g are parallel and the propagation is forward. Otherwise the propagation is backward.

¹⁸Wave propagation is allowed at ω_0 with infinite v_p but (non-zero) finite v_g .

¹⁹The term *balanced* does not mean *differential* in this context.

²⁰The guided wavelength is obviously different from that guided in the host line ($\beta \neq \beta_R$).

2.2.3 CL-Loaded and Resonant-Type Approaches

Because CRLH transmission lines are not readily available in nature, these structures have to be implemented by means of a host transmission line loaded with reactive elements (inductors, capacitors, and/or both of them in the form of resonators). Experimental CRLH lines were reported for the first time by Caloz et al. in microstrip technology [16], and by the Group of Eleftheriades in coplanar waveguide implementation [19]. The reactive elements responsible for backward propagation in both configurations were synthesized by semi-lumped²¹ components, such as series capacitive gaps and shunt metallic inductive strips (discrete commercial chip components can also be used instead [1]). This direct implementation is referred to as *LC network implementation* [1] or *CL-loaded approach* [3, 6]. Alternatively, transmission-line metamaterials featuring a CRLH behavior can also be built up by the so-called *resonant-type approach* [3, 6]. This realization consists of a host transmission line loaded with subwavelength resonators²² in combination with other reactive elements (inductors or capacitors), the typical resonant particles being split-ring resonators (SRRs) or other related topologies as those described in Sect. 2.3.²³ The first reported structure concerning this approach was proposed by Martín et al. [20], and it was conceptually based on and equivalent to the preceding Smith's LH structure shown in Fig. 2.3. Specifically, a coplanar waveguide (CPW) was periodically loaded with pairs of SRRs and signal-to-ground inductive strips (see Fig. 2.8). The SRRs were etched on the back side of the substrate, and underneath the slots of the CPW in order to enhance line-to-resonator magnetic coupling (this is the main coupling mechanism of SRRs as will be reviewed in Sect. 2.3.1 [21]). Another possibility to implement a CRLH response based on the resonant-type approach is by means of series capacitive gaps, and the complementary version (see Sect. 2.3.5) of the SRR, that is, the so-called complementary split-ring resonator (CSRR) [22, 23]. A chain of CSRRs provides a negative effective ϵ , while a negative effective μ is achieved through the gaps. Such a kind of line is illustrated in Fig. 2.9, where the CSRRs are etched in the ground plane of a microstrip line, beneath the signal strip, as strong line-to-resonator electric coupling (the dominant excitation field of CSRRs [21]) is achieved.

²¹Semi-lumped components are planar elements whose physical dimensions are usually restricted to be smaller than a quarter of wavelength. The components may also be designated to as lumped elements when the dimensions are smaller than one-eighth wavelength. These terminologies are in contrast to distributed (transmission line) elements in which the physical size is comparable to or larger than the wavelength [10, 18]. The advantage of electrically small planar (i.e. semi-lumped or even lumped) elements is that their behavior may be approximate by ideal (sizeless) lumped parameters using circuit theory.

²²Subwavelength resonators are those whose physical size is a small portion of the wavelength, and accordingly they may be referred to as semi-lumped or lumped resonators when composed of semi-lumped or lumped inductors and capacitors, respectively [18].

²³Note that CRLH lines based on the CL-loaded approach are also resonant by nature despite the fact that self-resonant elements are not used.

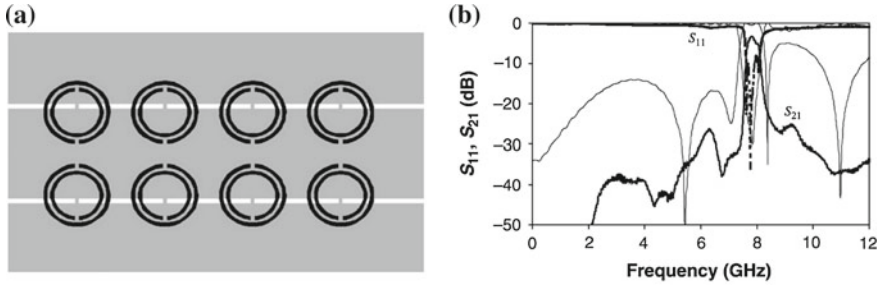


Fig. 2.8 CRLH transmission line based on SRRs and shunt inductive strips in coplanar waveguide technology. **a** Layout. **b** Simulated (*thin line*) and measured (*thick line*) frequency response. The passband is LH, since the CRLH line is not balanced and the RH passband is beyond the shown frequency range. Reprinted with permission from [20]

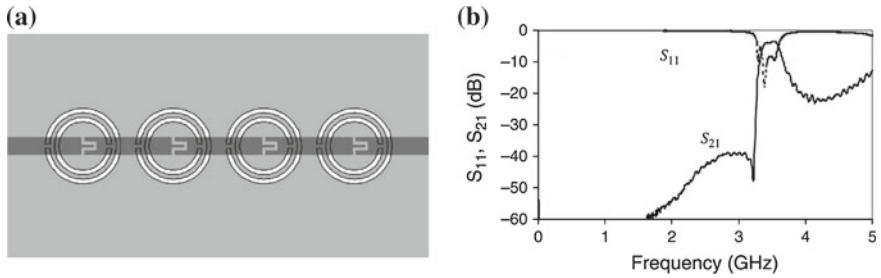


Fig. 2.9 CRLH transmission line based on CSRRs and series capacitive gaps in microstrip technology. **a** Layout reprinted with permission from [21]. **b** Measured frequency response reprinted with permission from [3]. The RH passband is outside the measured frequency range

Since the resonant-type approach employs subwavelength resonators, the individual unit cells can be modeled by lumped-element equivalent circuit models. However, the frequency response of a CRLH transmission line obtained by the resonant-type approach does not obey exactly the same behavior as the canonical²⁴ circuit of Fig. 2.6. Nevertheless, the corresponding models are qualitatively quite similar to the canonical one. The meaningful difference is the presence of a transmission zero on the left-hand side of the backward-wave band [3], which naturally is very useful in filtering applications. The first equivalent circuit models of SRR- and CSRR-based CRLH transmission lines were reported by Martín et al. [20] and Baena et al. [21], respectively, and these models were later revised and improved by Aznar et al. [24] and Bonache et al. [25], respectively. The main improvement is relative to the fact that by adding shunt strips (in SRR-loaded CPWs) and series gaps (in CSRR-loaded microstrip lines), the transmission zero is displaced, and this fact was not predicted by the initial models. None of these circuits models is shown here, but they are very similar to those of SNG transmission lines that will be presented in the next subsection.

²⁴Canonical refers to the simplest or standard form.

2.2.4 Resonant-Type Single-Negative Transmission Lines

A CRLH structure is intended to be used as a transmission line in the sense that only the passband/s is/are directly useful, the stopbands being usually parasitic effects [1]. Instead, structures exhibiting equivalent single negative (SNG) constitutive parameters are preferred to implement stopband responses (the structures involved in this thesis belong, in fact, to this category). One-dimensional resonant-type μ -negative (MNG) and ϵ -negative (ENG) structures can be synthesized artificially by merely loading a host line with SRRs and CSRRs, respectively. Signal propagation in these structures is inhibited in a narrow band in the vicinity of the resonance frequency of the resonators, whereas wave propagation is forward outside the forbidden band. Such a narrowband response is of course due to the self-resonant behavior of the loading particles. Consequently, these structures behave qualitatively as the canonical circuit models describing SNG transmission lines depicted in Fig. 2.5 only within a certain frequency range.

2.2.4.1 μ -Negative Coplanar Waveguides Loaded with Pairs of SRRs

Figure 2.10a shows the first proposed SRR-based μ -negative transmission line. It is the same structure as the CRLH line in Fig. 2.8a with the exception that the metallic strips are not introduced. Clearly the most relevant feature is that, by removing such strips, the backward passband in the vicinity of the SRR resonance frequency switches to a stopband response, as shown in Fig. 2.10b [20, 26].

In order to gain more insight into the transmission and reflection properties of SRR-loaded lines, the equivalent series reactance and shunt susceptance of a typical unit cell are plotted in Fig. 2.11a. The dispersion relation corresponding to an infinite structure obtained by cascading identical unit cells is shown in Fig. 2.11b. As can be observed, there is a stopband in the vicinity of the resonance frequency, f_0 , which occurs when the length of the unloaded line is a small fraction of the guided

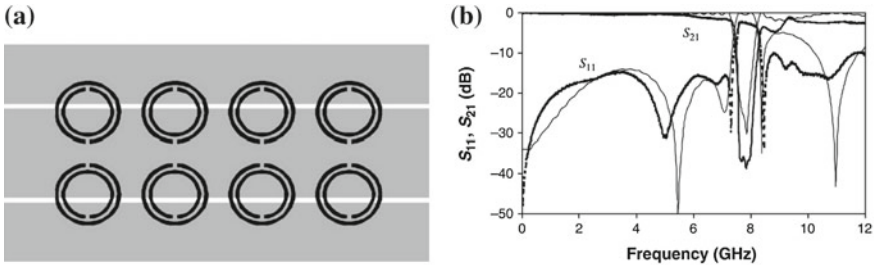


Fig. 2.10 MNG transmission line based on SRRs in coplanar waveguide implementation. **a** Layout. **b** Simulated (*thin line*) and measured (*thick line*) frequency response. Reprinted with permission from [26]

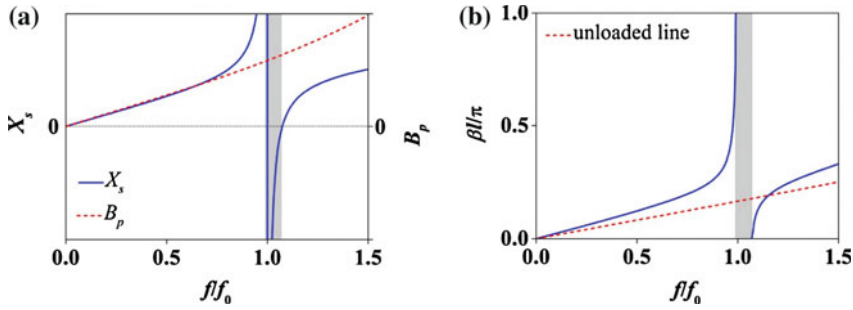


Fig. 2.11 Typical behavior of a unit-cell SRR-loaded transmission line. **a** Series reactance, X_s , and shunt susceptance, B_p , of an equivalent π -network extracted from electromagnetic simulation. **b** Dispersion diagram assuming an infinite periodic structure; the dispersion of the unloaded transmission line section is also shown. The stopband is highlighted in gray

wavelength (the dispersion for the considered transmission line section without the SRR is also shown). An analysis in terms of the impedances is as follows. Beyond f_0 , the series impedance is capacitive in a narrow band, and signal propagation is inhibited because the shunt impedance is also capacitive. However, the stopband region extends also below f_0 , despite the fact that the series and shunt impedances behave inductively and capacitively, respectively; the reason is that the series impedance attains extreme inductive values.²⁵ In relation to the constitutive parameters, the stopband has been associated to a negative μ in a narrow region above f_0 [21]. Within this frequency band the structure behaves as the canonical MNG transmission line shown in Fig. 2.5, since the structure is effectively homogeneous near this band ($\beta l = 0$ at the lower edge of the second propagating band). It is on occasions said that the stopband is also due to an extremely high positive μ in a narrow frequency range below f_0 . However, this statement is somewhat misleading in a strict sense, since as the series impedance becomes more and more inductive the operation regime goes away from the homogeneity condition ($\beta l \rightarrow \pi$).

Due to the small electrical dimensions of the SRRs at resonance, the behavior of SRR-loaded lines can be explained by the unit-cell equivalent-circuit model depicted in Fig. 2.12a. This circuit model was initially proposed by Martín et al. [20, 26], and later revised by Aznar et al. [24]. The per-section inductance and capacitance of the line are modeled by L and C , respectively, and the SRR is described by the resonant tank $L_s - C_s$ (see Sect. 2.3.1) that is magnetically coupled to the line through the mutual inductance M . This circuit can be simplified to the equivalent one depicted

²⁵Simultaneously positive or negative values of ϵ and μ are necessary and sufficient for wave propagation, as was illustrated in Fig. 2.1 (operation in the long wavelength regime is implicitly fulfilled). By contrast, the same sign of X_s and B_p (or different sign of X_s and $X_p = -1/B_p$) cannot guarantee wave propagation, unless the operation band is explicitly restricted to the long wavelength regime, as highlighted in Fig. 2.5. Note that possible impedance mismatch with feeding sources at the port terminals in practical situations resulting in reflections is not considered in the aforementioned assertions.

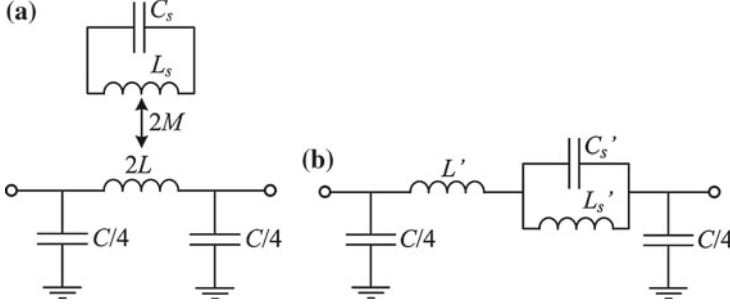


Fig. 2.12 Unit-cell equivalent-circuit model of an SRR-loaded CPW. **a** Model corresponding to half of the structure since a *magnetic wall* (open circuit) is applied along the longitudinally-oriented midplane by virtue of the symmetric topology and excitation mode (an even mode). **b** Equivalent transformed model using (2.9)

in Fig. 2.12b, provided that [3, 24, 27]

$$L' = 2L - L'_s, \quad (2.9a)$$

$$L'_s = 4C_s(\omega_0 M)^2 = 4\frac{M^2}{L_s}, \quad (2.9b)$$

$$C'_s = \frac{L_s}{4(\omega_0 M)^2} = \frac{C_s}{4} \left(\frac{L_s}{M} \right)^2, \quad (2.9c)$$

where

$$\omega_0 = \frac{1}{\sqrt{L_s C_s}} = \frac{1}{\sqrt{L'_s C'_s}} = 2\pi f_0, \quad (2.10)$$

is the angular resonance frequency of the SRR. Note that a zero in the transmission coefficient ($S_{21} = 0$) arises at this frequency, since the series branch is open-circuited. Therefore, the transformed circuit model clearly explains that the excitation of the SRR is responsible for returning the injected power to the source. Moreover, the lumped-element values of this circuit can be easily extracted systematically [28] (this procedure is used throughout this thesis). Finally, it should be noted that the circuit model converges to that of MNG transmission lines within a narrow bandwidth above resonance.

2.2.4.2 ϵ -Negative CSRR-Loaded Microstrip Lines

The first reported CSRR-loaded microstrip line is shown in Fig. 2.13a, which is the same as the one shown in Fig. 2.9a but with a uniform conductor strip (i.e. without the gaps). As can be seen in Fig. 2.13b, by removing the series gaps, signal propagation is inhibited in a narrow frequency band in the vicinity of the CSRR resonance frequency.

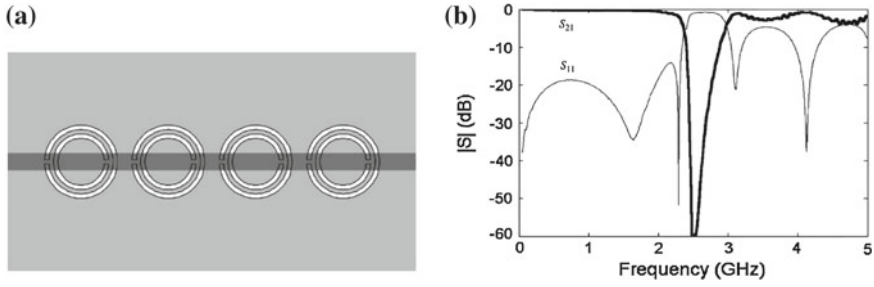


Fig. 2.13 ENG transmission line based on a CSRR-loaded microstrip line. **a** Layout and **b** measured frequency response. Reprinted with permission from [22]

In order to inquire into the propagation characteristics of CSRR-based transmission lines, the typical series reactance, shunt susceptance, and dispersion relation are plotted in Fig. 2.14. As can be observed, the stopband in the vicinity of the transmission zero frequency, f_z , is due to a shunt susceptance with negative ($f > f_z$) and extremely positive ($f < f_z$) values. Regarding the constitutive parameters, a CSRR-loaded line has been interpreted to behave in the stopband ($f > f_z$) as a 1D ϵ -negative metamaterial (where the structure may be viewed as the canonical ENG transmission line schematically depicted in Fig. 2.5) [21].

As long as the CSRRs are electrically small at their fundamental resonance, CSRR-loaded lines can be modeled by the lumped-element unit-cell circuit shown in Fig. 2.15 [21]. The CSRR is represented by the resonant tank $L_c - C_c$ (Sect. 2.3.5), and the per-section line inductance and capacitance are modeled by L and C , respectively. More specifically, C in reality accounts for the line-to-resonator electric coupling as this coupling can be modeled by connecting in series the line capacitance to the CSRR (see Appendix B.1). The extraction of the values of the circuit parameters

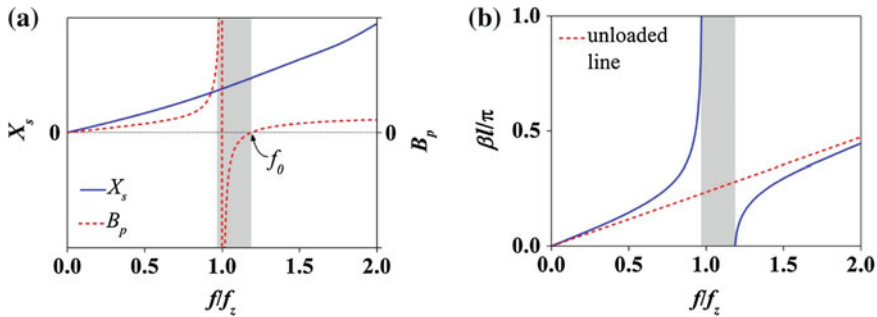


Fig. 2.14 Typical behavior of a unit-cell CSRR-loaded transmission line. **a** Series reactance, X_s , and shunt susceptance, B_p , of an equivalent T-network extracted from electromagnetic simulation. **b** Dispersion diagram for an infinite periodic structure; the dispersion of the unloaded transmission line section is also shown. The stopband is highlighted in gray

for a particular CSRR-loaded line is straightforward [29]. Inspection of this circuit model reveals that there is a transmission zero at a frequency

$$\omega_z = \frac{1}{\sqrt{L_c(C + C_c)}} = 2\pi f_z, \quad (2.11)$$

at which the shunt branch is short-circuited. Interestingly, the resonance frequency of the CSRR, given by

$$\omega_0 = \frac{1}{\sqrt{L_c C_c}} = 2\pi f_0, \quad (2.12)$$

occurs at a higher frequency than the transmission zero ($f_0 > f_z$).

Section 2.2.4 has been focused on SRR-loaded CPWs and CSRR-loaded microstrip lines. In these configurations, a significant component of the dominant excitation field (namely, magnetic in SRRs and electric in CSRRs) results parallel to the resonator axis.²⁶ Nonetheless, it is important to highlight that the corresponding circuit models and parameter extraction procedures are *general*. This means the models may be valid regardless of the resonator topology (Sect. 2.3) and the host line technology (e.g. CPW or microstrip) if the resonator is electrically small and coupled either magnetically (as the SRR) or electrically (as the CSRR) to the line. With regard to the circuit parameter extraction methodologies, despite the fact that they require the electromagnetic simulation of the structures, they are versatile in the sense that there is no restriction in the structures involved, in contrast to what usually occurs in analytical models. Therefore, the transmission and reflection characteristics of SRR- and CSRR-loaded lines are indeed somewhat general and may be extrapolated to other related structures.

In the light of Figs. 2.11a and 2.14a, it should be stressed that the proposed circuit models are able to mimic the behavior of SRR- and CSRR-loaded lines up to beyond the resonance frequency and the transmission zero frequency (the region of interest). In other words, the validity of the circuits is not limited to the long wavelength region.²⁷ To end this section, it is interesting to realize that the circuit models of SRR- and CSRR-loaded lines (Figs. 2.12 and 2.15) are formally dual circuits, that is, the series/shunt impedance of one of these models is proportional to the shunt/series admittance of the other circuit (compare Figs. 2.11a and 2.14a).²⁸ Hence, although SRR- and CSRR-loaded lines are not structurally complementary,²⁹ their corresponding behaviors manifest the duality property because the complementary resonators are illuminated by dual fields (this supports that the equivalent circuits

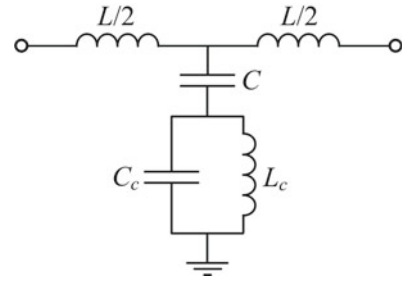
²⁶The electromagnetic field distribution of these lines is analyzed in Sect. 4.1.

²⁷The valid frequency range of the models is evaluated throughout the thesis by comparing circuit simulations with full-wave electromagnetic simulations and measurements.

²⁸Two networks are (formally and numerically) dual if $Z_{ii} = Y_{ii}$ and $Z_{ij} = -Y_{ij}$ ($i \neq j$), where Z_{ij} are the impedance matrix parameters of one network and Y_{ij} are the admittance matrix parameters of its dual one [18].

²⁹Besides the fact that complementary structures are defined in single planes, coplanar strips (CPS) are the complementary counterpart of a CPW.

Fig. 2.15 Unit-cell equivalent-circuit model of a CSRR-loaded microstrip line



may be independent of the technology of the host transmission line). Thus, the dispersion relation of SRR- and CSRR-loaded lines is the same (at least qualitatively as is apparent from Figs. 2.11b and 2.14b), a property derived from dual circuits. When formally dual circuits are also numerically exact dual, their dispersion relation is exactly the same (Appendix A).

2.2.5 Discussion About Homogeneity and Periodicity

Homogenization in metamaterials means that the homogeneity condition is achieved in the vicinity of the operating frequency. As has been shown, the transmission-line approach of metamaterials characterizes the electromagnetic properties of homogeneous transmission-line metamaterials by either effective constitutive parameters or immittances.³⁰ However, this description is limited to the long wavelength regime, and cannot be extended to frequencies where the wavelength becomes comparable to the period. Obviously, such a restriction may mask and forbid useful functionalities, since some interesting phenomena occur outside the long wavelength regime. Contrarily, the propagation constant as well as the characteristic impedance of periodic structures (including transmission-line metamaterials) can be defined rigorously at all frequencies using the powerful classical theory of periodic structures [30] (Appendix A), without invoking the theory of effective-medium approximation. Therefore, from an engineering standpoint, periodic metamaterial structures are usually characterized by their propagation constant and characteristic impedance rather than by their effective permittivity and permeability [1, 3, 4].

In general, the synthesis of LH (or CRLH) devices is usually referred to as *dispersion and impedance engineering* [3, 4, 6] since the relevant parameters are the electrical length and the characteristic impedance. Indeed, for the design of circuits and components, homogeneity is irrelevant to tailor the electrical length and the impedance. Furthermore, these devices are commonly composed of a single unit

³⁰Immittances are either impedances or admittances [18].

cell³¹ toward miniaturization, leading to indisputably inhomogeneous structures. With respect to stopband structures (SNG-based), by sacrificing homogeneity, significant signal rejection may be achieved within a determined forbidden band by a few periods, making unnecessary a large structure composed of many cells.

To sum up, the design of devices in the RF/microwave community is not usually focused on the implementation of effectively homogeneous transmission lines, but on taking advantage of their high controllability in the response, and/or their small electrical size. When the effective-homogeneity condition is not satisfied and/or there are not many cells, these devices cannot be strictly considered as metamaterials. However, as suggested by Martín et al. [6] and Aznar et al. [31], the definition of metamaterial transmission lines is not usually restricted to those exhibiting homogeneity and periodicity or quasi-periodicity (contrary to the definition given at the beginning of Sect. 2.2). Consequently, terms such as *transmission-line metamaterials*, *metamaterial transmission lines*, *metamaterial-based lines*, *metamaterial-inspired lines*, or even *metalines*, are often used in a broad sense to describe artificial transmission lines based on metamaterial concepts, ignoring whether effective homogeneity and periodicity are accomplished or not.³²

2.3 Metamaterial-Based Resonators

This section analyzes several resonator topologies in the form of split rings³³ employed for the synthesis of metamaterials, transmission-line metamaterials, or RF/microwave devices inspired by metamaterials. These resonators are often known as *metamaterial-based resonators* or simply *metamaterial resonators*. Indeed, negative permeability/permittivity structures may be implemented by means of topologies different from that of the original SRR³⁴/CSRR. The additional considered resonant elements are *strip* (made of an arrangement of metals) as well as *slot* (engineered apertures in a metallic plane) resonators. Many electrically small planar resonators have been reported in the literature [3, 5, 6], and they can be classified according to several criteria. The list is limited here to those split ring type resonators that are used throughout this thesis. All of them have in common the following features:

- *Subwavelength*, and accordingly they may be referred to as semi-lumped or lumped resonators.
- *Closed*, in the sense that resonance is induced by external electromagnetic fields.³⁵

³¹The propagation constant and the characteristic impedance obtained from the theory of periodic structures is still valid for a single unit cell.

³²Besides the broad definition, a distinction between metamaterial-based and metamaterial-inspired has been proposed [32].

³³*Split rings* are also sometimes called *open rings* [33].

³⁴*SRR* is exclusively used here to designate the original split-ring resonator topology [13].

³⁵On the contrary, *open* split-ring resonators have well-defined port terminals, e.g. the open split-ring resonator (OSRR) [34] or the open complementary split-ring resonator (OCSRR) [35].

- *Planar*, being fully compatible with planar technology.
- *Symmetric*, so that when the topology is bisected along its symmetry plane, one of the halves is the mirror image of the other half (a plane of symmetry acts as a mirror). Additionally, resonators having two symmetry planes are said to be *bisymmetric*.

However, all the topologies exhibit different peculiarities that make them useful or more appropriate in some circumstances. The main purpose of this section is to gain insight into the electromagnetic characteristics and the equivalent circuit models of the resonators derived from symmetry properties (a discussion about different alternatives for the synthesis of metamaterial structures is not provided). With a view to doing so, the SRR topology still holds special attention because of its relevance.

The most basic assumption in effective media theory (Sect. 2.1) is that homogenization (averaging) makes sense only if the variation of the average field is small at the scale of the period [3, 13]. The validity of homogenization is usually expressed in terms of the size of the elements forming the discrete medium, so that they must be small as compared with the wavelength. It is assumed here that the size of the resonators is on a scale much shorter than the wavelength, such that an average value for the fields may be sensibly defined. Thus, the resonators are supposed to be illuminated by external uniform (i.e. spatially constant in magnitude and phase) time-varying electric or magnetic fields with the customary sinusoidal, or harmonic, time dependence $e^{j\omega t}$.

2.3.1 Split-Ring Resonator (SRR)

The split-ring resonator (SRR) consists of two metallic concentric and coupled split rings with slits on opposite sides, as depicted in Fig. 2.16a. Although there are some precedents in the scientific literature related to split-ring resonators [5, 36], this specific topology was proposed by Pendry et al. [13] to build up for the first time a negative permeability medium [12].

When the rings are excited by an external time-varying magnetic field directed along the axial direction (z -oriented), an electromotive force around the rings is generated that, in turn, induces currents in the rings. The slit (or gap) in each ring prevents current from flowing around the individual rings, so that the slits force the electric current to flow from one ring to the other through the inter-ring slot, taking the form of a displacement current (see Fig. 2.16b). As is apparent from Figs. 2.16b and 2.17, the symmetry plane (xz -oriented) behaves as a virtual *electric wall*. The current loops induce a magnetic dipole moment along the resonator axis (z -orientation). Additionally, an electric dipole moment is also generated in the plane of the particle, oriented orthogonally to the plane of symmetry (y -direction).³⁶

³⁶The radiation of split-ring resonators can be quantified by the induced dipole moments through an equivalent radiation resistance. Nevertheless, since the dimensions of the dipoles are small relative to the wavelength, in general radiation may be neglected [5, 37].

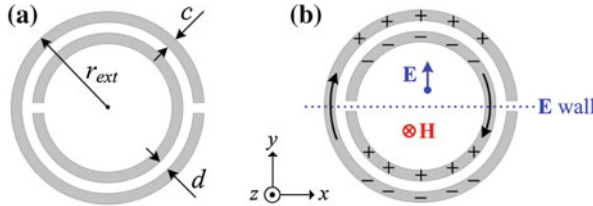


Fig. 2.16 Symmetric split-ring resonator (SRR). **a** Circular topology. **b** Fundamental resonance: orientation of the polarization fields, sketch of the charge distribution and currents, and boundary condition at the symmetry plane

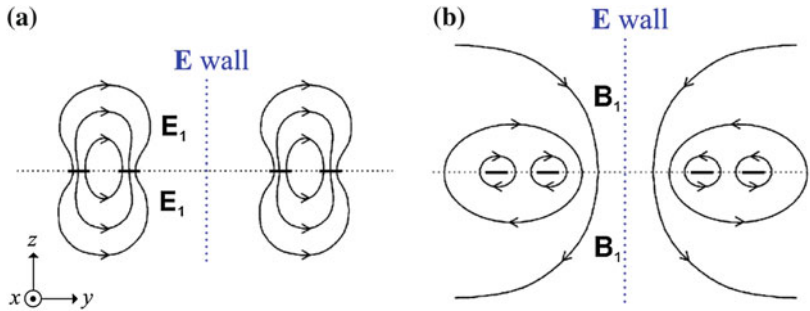


Fig. 2.17 Sketch of the electric **a** and magnetic **b** field distributions at the SRR fundamental resonance frequency. Reprinted with permission from [21]

By symmetry, the electric charges in the upper half of the SRR are the images of the charges in its lower half, and two parallel electric dipoles are generated on each half. This means that a time-varying electric field is also able to excite the SRR, inducing a charge density in the form of an electric dipole that causes currents to flow. When there is present an/a electric/magnetic dipole in a metamaterial resonator, the particle is said to be electrically/magnetically polarized.³⁷ Since both an electric dipole and a magnetic dipole are induced, the SRR suffers from cross-polarization effects, so that it may become electrically polarized as a response to an applied magnetic field, and vice versa [5, 38]. This property may also be derived from the fact that the SRR is not invariant by inversion, since any resonator without inversion symmetry with regard to its center must exhibit some degree of cross-polarizability [3].³⁸ However, although the SRR shows simultaneously magnetoelectric response at resonance, the magnetic field has been found to be the dominant excitation mechanism [21, 39, 40].

³⁷Polarization is related here to the generation of local (microscopic) dipole moments in the presence of external fields (like medium electric and magnetic polarizations accounted for by ϵ and μ , respectively, at the macroscopic level), and not to wave polarization.

³⁸A bidimensional object possesses inversion symmetry when is invariant by rotating 180° taking its center as the rotation axis.

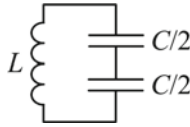


Fig. 2.18 Equivalent circuit model of an SRR. The total capacitance across the slot between the rings is C , which is divided into two series components corresponding to the two identical halves of the resonator ($C = 2\pi r_0 C'$, where C' is the per-unit-length capacitance along the slot and $r_0 = r_{ext} - c - d/2$ is the mean radius). The SRR behaves as an externally driven LC resonator

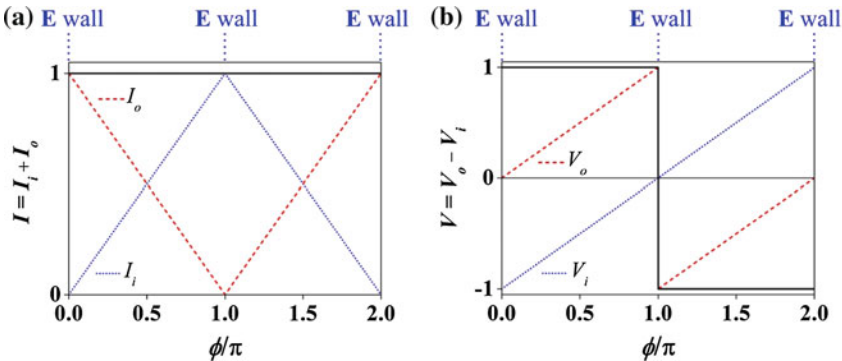


Fig. 2.19 Angular dependence of the quasistatic current and voltage in the SRR; the inner ring is cut at $\phi = 0$. The subscripts i and o stand for the inner and outer rings, respectively. **a** Normalized current distribution; the total current in both rings taken as a summation is constant. **b** Normalized voltage distribution; the voltage across the two rings in each half is constant

As long as the perimeter of the SRR is electrically small with regard to a half-wavelength,³⁹ a quasistatic analysis is plausible which eases the analysis of the resonator. Under the quasistatic approximation, the behavior of the SRR can be modeled as a self-resonant closed LC circuit as that shown in Fig. 2.18 that may couple to external electromagnetic fields [38]. The inductor L represents the self-inductance of the SRR and the capacitor C stands for the capacitance between the rings. Analytical expressions for L and C have been reported in the literature [3, 38]. In this quasistatic model, the capacitance associated to the slits of the rings is neglected, since most of the electrostatic energy is located between the rings [13]. It is worth mentioning that a more detailed circuit model with distributed elements and taking into account the gap capacitance was later reported [41, 42]. The two gap capacitances, produced by the accumulation of electric charges, can be regarded as being added in parallel to the inter-ring capacitance. It was shown that such a distributed model converges to the quasistatic model when the gap capacitances are neglected and the electrical length of the SRR is small.

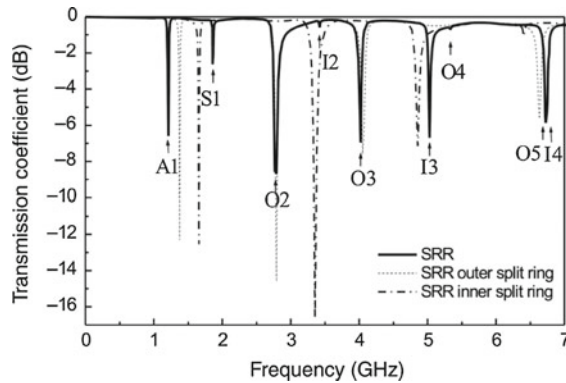
Figure 2.19 shows the quasistatic distribution of voltage and current. On each ring, currents vanish at the slits because the gap capacitance is disregarded, whereas

³⁹The overall size of the SRR is typically about one-tenth of the wavelength [3].

currents attain maximum values at the center of the rings (namely, $\phi = 0$ for the outer ring and $\phi = \pi$ for the inner ring). Given that the SRR is electrically small, currents on each ring are supposed to vary linearly midway between these extreme values (this results in a triangular current distribution). Nonetheless, the total current on the SRR taken as the sum of the individual currents is uniform around its perimeter. Hence, the whole SRR behaves as a small closed loop of uniform current whose self-inductance can be calculated as the average inductance of the two rings, i.e. as the inductance of a single closed loop with identical width to that of the individual rings (c) and identical mean radius (r_0) [38]. With respect to the voltage distribution, it also exhibits a linear variation in each ring. However, the voltage difference across the slots is constant in each half of the SRR, and the slot between the rings may be modeled by two series capacitances (associated to each half) that store the same amount of charge (but of opposite sign) at both sides of the slot. As expected, the voltage distribution is anti-symmetric with regard to the symmetry axis ($\phi = 0$ and π). Therefore, the voltage is zero at the symmetry plane since a virtual short circuit (an electric wall) appears along this plane.

It is also interesting to analyze the SRR fundamental resonance from the theory of coupled resonators [18]. When the mean circumference of a closed ring resonator is equal to an integral multiple of the wavelength, resonance is established [33]. By cutting the ring by a split, the resulting resonator is essentially a distributed open-circuited half-wavelength resonator with a (weak) loading capacitance at the open end. Since the inner and outer rings of the SRR are not identical, their self-resonances are different from each other. By coupling these half-wavelength rings, the lower resonance frequency (associated to the outer ring) shifts downward, giving rise to quasistatic conditions as a first-order approximation (see Fig. 2.20). For such a reason, the first (or lowest) resonance frequency is referred to as the *fundamental* or *quasistatic* resonance frequency. Obviously, SRRs (and all the other considered resonators) exhibit higher-order resonances that can be excited at higher frequencies (Fig. 2.20). These higher-order resonant modes (beyond the scope of this thesis) are

Fig. 2.20 Quasistatic (identified as A1) and some dynamic resonance frequencies of an SRR. The resonances correspond to transmission zeros in the transmission coefficient of an SRR-loaded microstrip line. Reprinted with permission from [43]



referred to as *dynamic* resonances, since non-uniform total currents are induced and the particle is thus no longer electrically small [3, 43].

2.3.2 Double-Slit Split-Ring Resonator (DS-SRR)

The double-slit split-ring resonator (DS-SRR) is derived from the original topology of the SRR by introducing an additional cut in each ring and by rotating one of the rings 90° , as shown in Fig. 2.21a [44]. This particle is bisymmetric, which means that it possesses two orthogonal symmetry planes, resulting invariant by inversion. As Fig. 2.21b depicts, the two symmetry planes behave as electric walls at resonance and, in virtue of their orthogonality, the appearance of a net electric dipole is prevented. As a result, the fundamental resonance of the DS-SRR cannot be electrically excited with uniform fields. Contrarily, an axial (z -direction) time-harmonic magnetic field can establish resonance inducing a magnetic dipole moment. Therefore, this particle does not exhibit cross polarization.

In comparison to the original SRR, by applying a quasistatic analysis, the DS-SRR has almost the same inductance but four times smaller capacitance (provided that the overall dimensions of the resonators are the same). The reduction in the total capacitance arises from the series connection of the four capacitances, each of them corresponding to each quadrant (see Fig. 2.22). As a consequence, the resonance frequency of the DS-SRR is about twice that of the SRR, and the electrical size as well (in fact this is likely to be expected because the length of the individual split

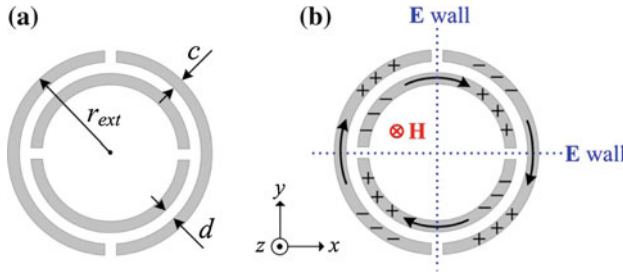
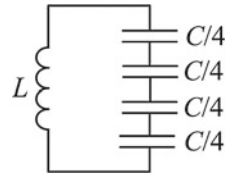


Fig. 2.21 Bisymmetric double-slit split-ring resonator (DS-SRR). **a** Circular topology. **b** Fundamental resonance: orientation of the polarization fields, sketch of the charge distribution and currents, and boundary conditions at the symmetry planes

Fig. 2.22 Equivalent circuit model of a DS-SRR. The total capacitance, $C = 2\pi r_0 C'$, is divided into the four quadrants



rings has been decreased by a factor of two). Accordingly, although the equivalent circuit model of the DS-SRR is formally the same as that of the SRR, the description of the electrical behavior of the particle by the model is less accurate for the DS-SRR.

2.3.3 Folded Stepped-Impedance Resonator (FSIR)

Stepped-impedance resonators (SIRs) are common planar building blocks in microwave engineering [45]. SIRs are essentially open-ended resonators where the width of the strip is varied abruptly. It is well known that a tri-section SIR can be made electrically small (as compared to a uniform half-wavelength resonator) by narrowing the central section and widening the external ones. Further miniaturization can be achieved by folding the SIR, as depicted in Fig. 2.23a. The fundamental resonance frequency of the folded SIR (FSIR) can be excited by time-harmonic electric (y-direction) and/or magnetic (z-orientation) fields. Hence, cross-polarization effects are present, and both an electric dipole and a magnetic dipole are induced. At the plane of symmetry, an electric wall boundary condition is established. Figure 2.23b illustrates all the above-cited properties at resonance.

In terms of electric circuit parameters, basically, the inductive component of the particle is directly related to the inductance of the narrow strip (w_2), while its capacitance is provided by the wide sections (w_1) and the gap (s). Thus, an FSIR may be regarded as a planar implementation of a capacitively-loaded loop. As a consequence, the equivalent circuit model of an FSIR (see Fig. 2.24) is qualitatively the same as that of an SRR.

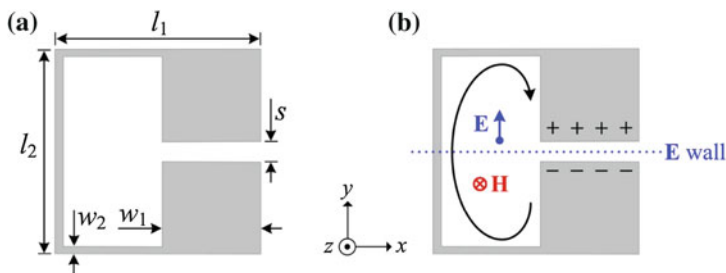
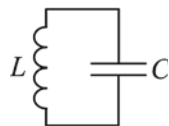


Fig. 2.23 Symmetric folded stepped-impedance resonator (FSIR). **a** Square topology. **b** Fundamental resonance: orientation of the polarization fields, sketch of the charge distribution and currents, and boundary conditions at the symmetry plane

Fig. 2.24 Equivalent circuit model of an FSIR



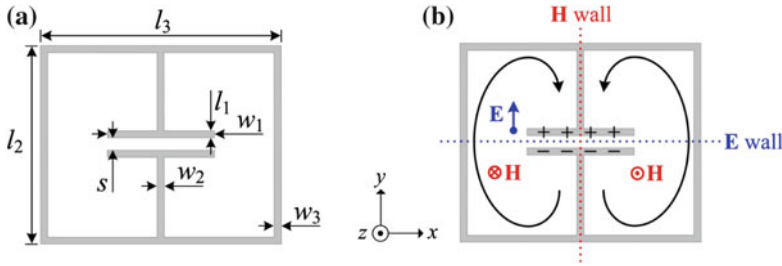


Fig. 2.25 Bisymmetric electric inductive-capacitive (ELC) resonator. **a** Rectangular-shaped topology. **b** Fundamental resonance: orientation of the polarization fields, sketch of the charge distribution and currents, and boundary conditions at the symmetry planes. Since in this thesis the ELC is magnetically coupled to transmission lines, the resonator excitation by contra-directional magnetic fields is also illustrated

2.3.4 Electric Inductive-Capacitive (ELC) Resonator

The so-called electric-field-coupled inductive-capacitive (ELC) resonator (or simply electric-*LC* resonator) was proposed by Schurig et al. [46] as an alternative to metallic wires for the implementation of negative permittivity (ENG) media. As illustrated in Fig. 2.25a, the ELC resonator is a bisymmetric planar structure consisting of a pair of mirrored capacitively-loaded metallic loops in contact. Clearly, this particle can be viewed as two combined (merged) FSIRs.

As indicated in Fig. 2.25b, besides an electric wall, the ELC resonator exhibits a *magnetic wall* in an orthogonal plane at the fundamental resonance. At this resonance, the current flows through the central branch so that the (instantaneous) current is clockwise in one loop and counterclockwise in the other one, giving rise to a net displacement current across the gap. In consequence, the opposite magnetic moments originated by the two current loops cancel out and prevent the presence of a net axial magnetic dipole moment (z -direction). For such a reason this resonator cannot be driven by means of a uniform axial time-varying magnetic field.⁴⁰ On the other hand, an electric dipole moment is still present in the plane of the particle directed along the gap (y -oriented), which means that this resonator can be excited through a uniform time-harmonic electric field applied to that direction. As a result, cross polarization does not affect the ELC resonator, a property that can also be inferred because of its inversion symmetry inherent to its bisymmetry.

The equivalent circuit model of an electrically small ELC resonator is schematically depicted in Fig. 2.26 [46]. As in the FSIR, the narrow section of each loop (w_2 and w_3) is associated to an inductance, while the wide section (w_1) and the gap (s) are modeled by a capacitance. Therefore, the ELC resonator is in essence an

⁴⁰Nevertheless, the particle may be magnetically excited if the applied magnetic fields in the individual loops are in opposite directions to each other. In fact, in this thesis the ELC resonator is magnetically coupled to transmission lines.

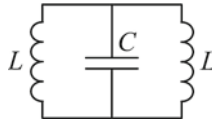


Fig. 2.26 Equivalent circuit model of an ELC resonator. Mesh currents must flow into the same direction through the capacitor for resonance establishment

electrically-coupled LC resonator (i.e. an electric resonator) under uniform fields, as its terminology suggests.

2.3.5 Complementary Resonators

The complementary counterparts of the resonators analyzed in the preceding subsections are presented here. As is well known, two complementary structures are defined as those where one is obtained from the other by exchanging the apertures (slots) for the solid (metallic) parts of a plane [47]. Therefore, when complementary structures are combined, they form a single infinite solid screen with no overlaps. As suggested in the literature [48], to avoid ambiguity, a resonator made of electrically conducting strips is referred here to as a *strip resonator*, whereas a resonator obtained by cutting slots in a metallic surface as a *slot resonator*.

With a view to analyzing the behavior of resonators in the form of slots, the concepts of duality and complementarity are invoked as often [47, 48]. Electromagnetic duality (often referred to as Babinet's Principle) means that Maxwell's equations possess duality in electric and magnetic quantities; the mathematical solution for an electromagnetic field is identical to that for its dual one obtained by a suitable interchange of electric and magnetic quantities. The dual of a strip resonator can be mathematically obtained by the definition of fictitious magnetic conductors. In practice, a physical dual is implemented by a slot resonator. Thus, strip and slot resonators are the physical implementation of dual problems. It follows that, the electromagnetic fields of complementary structures are identical with the exception of a constant and that the electric and magnetic fields are interchanged. Therefore, the electric/magnetic field distribution of a planar slot structure is the same as the magnetic/electric field distribution of a planar strip structure (the sign of the dual field, however, must change on each side of the slot structure in order to satisfy the boundary conditions in the plane of the particle). It is also well known that the impedance and admittance of complementary structures are proportional, and accordingly their resonance frequencies are identical. Another interesting property derived from duality is that complementary periodic structures have exactly the same dispersion curve [9]. A case study on this matter will be addressed in Sect. 2.4.

It should be pointed out that duality in complementary structures strictly applies to infinite, planar, zero thickness, and perfectly conducting electric screens [47].

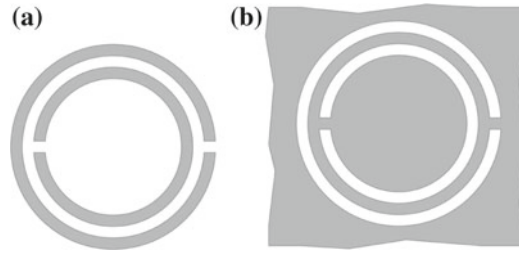


Fig. 2.27 Complementary resonators. **a** SRR and **b** CSRR

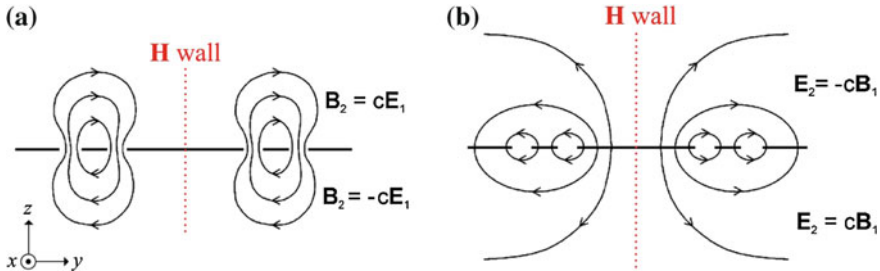


Fig. 2.28 Sketch of the magnetic **a** and electric **b** field distributions at the CSRR fundamental resonance frequency. The field distributions of the CSRR and SRR are dual, c being the velocity of light. Reprinted with permission from [21]

Although in practice such ideal conditions cannot be fulfilled, for very thin good conductors and metallic planes substantially larger than the wavelength and the slot region, Babinet's Principle predicts the actual behavior to a high degree [37]. One of the most relevant discrepancies due to deviations from ideal conditions is a shift in the resonance frequency.

Let us consider as an illustration the complementary screen of the SRR, i.e. the complementary split-ring resonator (CSRR) [22], as shown in Fig. 2.27.⁴¹ The electromagnetic field distribution at the fundamental resonance of the CSRR is sketched in Fig. 2.28. It is apparent that the electric and magnetic fields in the vicinity of the CSRR are the dual fields of those of the SRR (see Fig. 2.17), since the roles of the electric and magnetic fields are interchanged. Thus, at the symmetry plane of the CSRR, a magnetic wall arises. The induced electric and magnetic dipoles are also dual, as illustrated in Fig. 2.29 [23]. While the SRR behaves as an axial magnetic dipole and an electric dipole in the plane of the rings, the CSRR (when is seen from one side) exhibits an axial electric dipole and a magnetic dipole in its plane. Note that the dipoles point toward opposite directions on the two sides ($z < 0$ and $z > 0$) of the CSRR. Therefore, the net electric and magnetic dipoles generated by the CSRR become zero. This ensures that both the total magnetic polarization parallel to the screen (y -axis) and the total electric polarization perpendicular to the screen (z -axis)

⁴¹Despite the nomenclature, the SRR is the complementary of the CSRR as well.

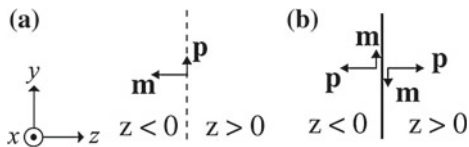


Fig. 2.29 Induced electric (p) and magnetic (m) dipoles by the **a** SRR and the **b** CSRR [23]. The resonators lie in the plane $z = 0$. No net dipoles are induced in the CSRR seen from both sides

vanish, as it must be for a metallic plane (electric currents in a plane can produce only net tangential electric moments and normal magnetic moments) [3]. As a consequence, when referring to slot resonators, uniform and temporally varying fields are applied to only one side. The CSRR can thus be excited by an axial electric field and/or a magnetic field polarized in the direction orthogonal to its symmetry plane, as depicted in Fig. 2.30a. Hence, cross-polarization effects are also present in the CSRR, the electric field being the main driving mechanism [21].

Figure 2.30 shows the results after applying duality to all the considered resonators. The complementary of the DS-SRR is called double-slit complementary split-ring resonator (DS-CSRR) [44]. Like the SIR, its complementary counterpart [49] has been extensively used in the last decade in the microwave community, and it is referred to as dumbbell-shaped defected ground structure (DGS)⁴² here, as it is often called in the literature. Neither the unfolded nor the folded dumbbell DGS is used in the present thesis, but it is included here for completeness. The physical dual of the ELC resonator has been called magnetic-LC (MLC) resonator for coherence throughout this thesis, meaning that uniform fields are able to excite its fundamental resonance only by magnetic fields (the MLC is therefore a magnetic resonator). An alternative denomination in the literature is complementary electric-LC (CELC) resonator [50].

Finally, it may be shown that electromagnetic duality implies circuit theory duality. Consequently, any planar structure and its complementary screen are dual in circuit theory as well [51]. Thus, the equivalent circuit models of slot resonators may be inferred by the dual circuits of the models corresponding to the strip resonators. By applying circuit duality, inductances are replaced with capacitances, and series-connected circuit elements become parallel-connected circuit elements. The equivalent circuit models for the CSRR and the DS-CSRR are represented in Fig. 2.31 [21]. The capacitance of the CSRR may be calculated as the capacitance of a disk of radius $r_0 - c/2$ ($r_0 = r_{ext} - c - d/2$) surrounded by a metal plane at a distance c of its edge (analytical expressions have been derived [21]). The CSRR inductance is given by the parallel combination of the two inductances connecting the inner disk to the outer metallic region of the CSRR. Such inductances may be calculated as the inductance of a CPW with a strip width d and slot width c . A circuit model of the MLC resonator was developed by Naqui et al. in [52], while the circuit of the folded dumbbell-shaped DGS can be readily derived from that circuit.

⁴²A slot resonator is sometimes referred to as a *defected ground structure* (DGS) or *patterned ground structure* (PGS) when it is etched in the ground plane.

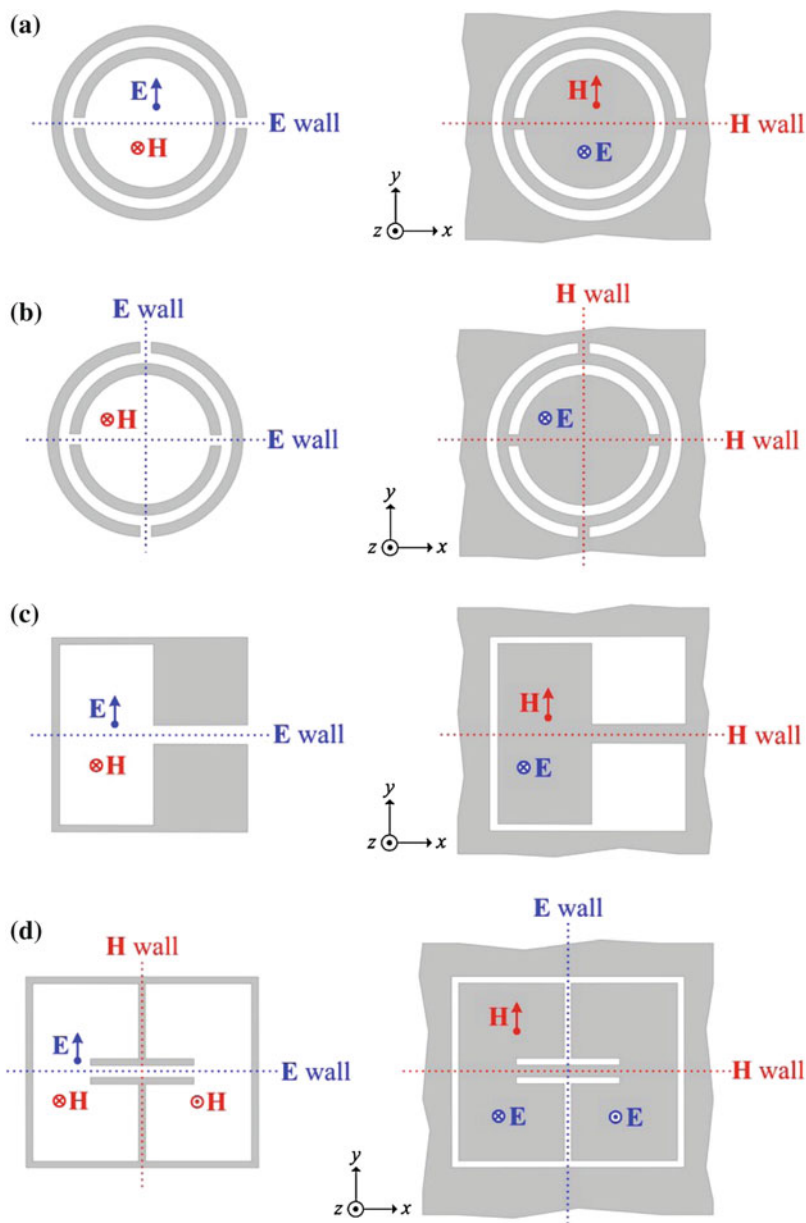


Fig. 2.30 Polarization fields and boundary conditions at the symmetry planes at the fundamental resonance in complementary split-ring resonators by applying duality

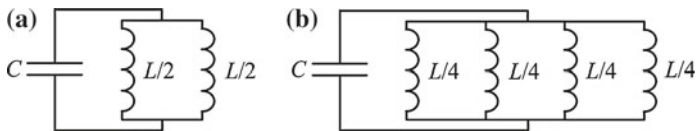


Fig. 2.31 Equivalent circuit model of a **a** CSRR and a **b** DS-CSRR. The total inductance, $L = 2\pi r_0 L'$, is divided into equal parallel contributions, where L' is the per-unit-length inductance of an equivalent CPW

2.4 Magneto- and Electro-Inductive Waves

This section is devoted to propagating structures based on inter-resonator coupling. Indeed, metamaterial resonators may be excited not only, for instance, by a transmission line, but also by coupling them. Without loss of generality, imagine periodic chains of either SRRs or CSRRs, as depicted in Fig. 2.32. Since these two arrays complement to one another to form a solid screen, both structures exhibit numerically the same dispersion relation [9], as mentioned in Sect. 2.3.5. However, it is apparent from duality that the nature of the propagation in the two arrays must somehow interchange dual variables. As will be argued, planar arrays of SRRs and CSRRs are able to guide backward *magneto-inductive waves* and *electro-inductive waves*, respectively.

2.4.1 Magneto-Inductive Waves in Arrays of Magnetically-Coupled Resonators

Magneto-inductive waves (MIWs) were first reported and studied in the frame of metamaterial science by Shamonina et al. [53, 54], and many works have been pub-

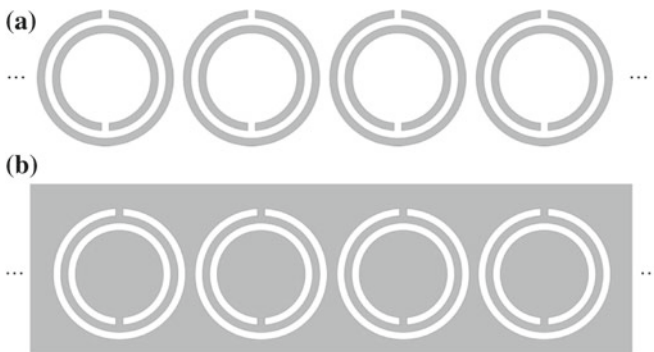


Fig. 2.32 Periodic array of coupled **a** SRRs and **b** CSRRs through which dual magneto- and electro-inductive waves may arise, respectively

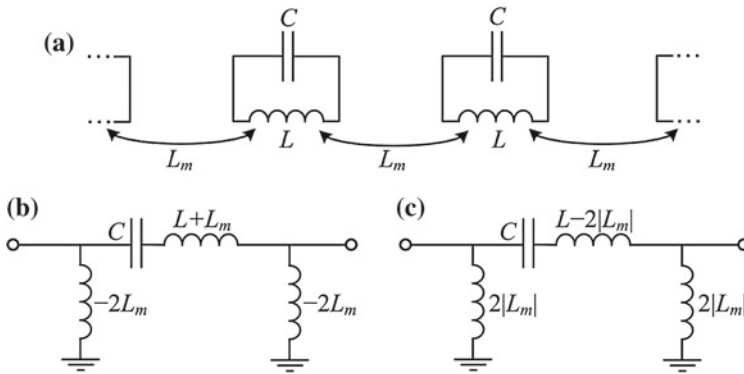


Fig. 2.33 Equivalent circuit of a periodic magneto-inductive waveguide assuming magnetic interaction only between adjacent resonators. **a** Circuit with mutual inductance. Unit-cell transformed circuits (see Appendix B.2) for an **b** axial and a **c** coplanar arrangement of resonators supporting forward and backward waves, respectively

lished subsequently [5, 55, 56]. MIWs are a form of guided waves which propagate through an array of magnetically-coupled resonators that acts as a waveguide. A lumped-element circuit representation of a periodic magneto-inductive waveguide is illustrated in Fig. 2.33a. Each resonator is modeled by an inductance L and a capacitance C , and is coupled to its nearest neighbor⁴³ by a mutual inductance L_m . Thus, the term *magneto-inductive wave* originates from the fact that such waves arise due to voltages induced by magnetic coupling between the resonant elements [57]. The propagation of MIWs occurs within a narrow passband around the resonance frequency of the isolated elements, i.e. $\omega_0 = 1/\sqrt{LC}$, and the associated bandwidth is dependent on how strongly the resonators are coupled to each other. The stronger the interaction between the elements, the wider the passband of the MIWs [57]. Both forward and backward MIWs may exist, depending on the sign of the mutual inductance between resonators (see Fig. 2.33b, c). While mutual inductance is positive in an axial configuration, it is negative when the resonators are arranged in a coplanar configuration since the magnetic field originating in one resonator crosses another one in the opposite direction [54].

MIWs are expected to be present in whatever chain of resonant elements that can be described by LC resonant tanks, as long as the coupling between them is magnetic [54, 58] or dominantly magnetic in the presence of negligible mixed magnetoelectric coupling [3]. The first magneto-inductive waveguide was studied in the form of a theoretical periodic array of magnetically-coupled capacitively-loaded loops, as can be seen in Fig. 2.34a for a coplanar arrangement [54]. The corresponding dispersion diagram assuming that coupling is restricted to the nearest neighbors is shown in

⁴³The first-neighbor approximation assumes that the field strength declines so rapidly away from a resonator that it is too small beyond the nearest neighbor. The accuracy of this first-order coupling is dependent on the resonant elements [3, 5] and the spacing between resonators.

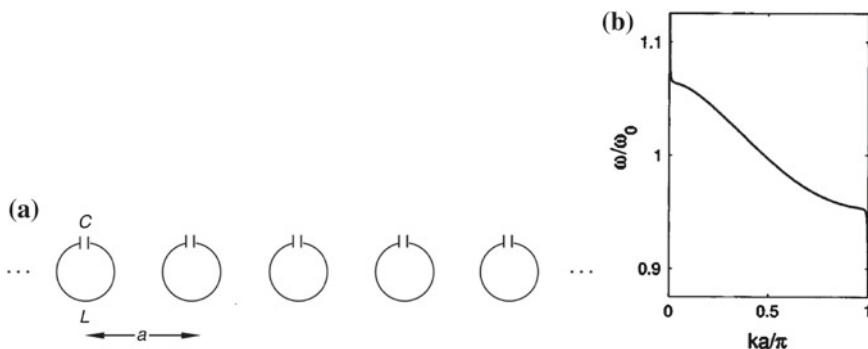


Fig. 2.34 Backward magneto-inductive waves in an array of coplanar capacitively-loaded loops. **a** Theoretical layout reprinted with permission from [59]. **b** Dispersion relation with nearest neighbor coupling reprinted with permission from [54]

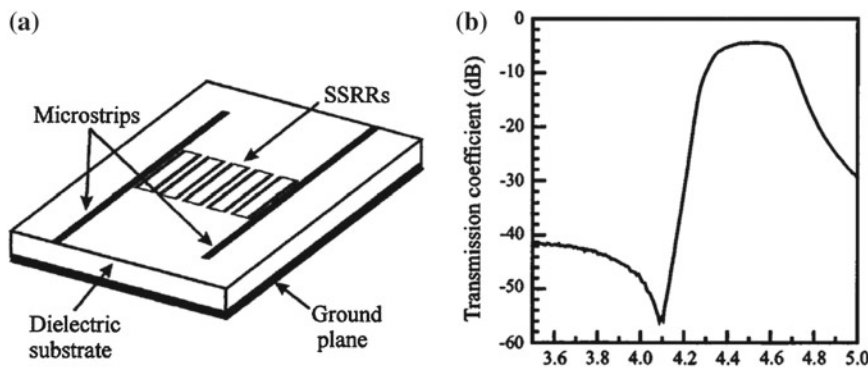


Fig. 2.35 Backward magneto-inductive waves in an array of split-ring resonators in coplanar configuration in microstrip technology. **a** Layout; the input/output SSRRs are coupled to input/output microstrip lines. **b** Measured transmission coefficient. Reprinted with permission from [58]

Fig. 2.34b, where the backward wave nature is clearly visible. Shortly after, MIWs were also excited in a periodic arrangement of split squared ring resonators (SSRRs), as shown in Fig. 2.35 [58]. This type of split-ring resonator (not described in Sect. 2.3) is not symmetric, but it does not suffer from cross-polarization effects as it exhibits inversion symmetry.

It is also worth mentioning that MIWs belong to the category of slow waves, since its phase velocity may be orders of magnitude smaller than the velocity of an electromagnetic wave propagating in the same medium [3, 6].⁴⁴ Since slow-wave structures are of interest in device miniaturization, and bandpass characteristics are useful in signal filtering, MIWs have found many diverse applications. Some

⁴⁴Slow-wave effects are usually accounted for by the resulting phase velocity reduction factor (or slow-wave factor).

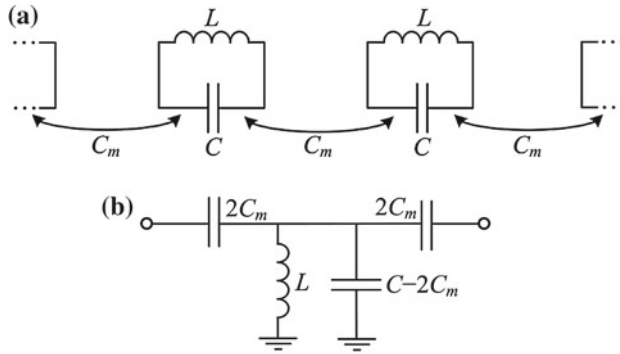


Fig. 2.36 Equivalent circuit of a periodic electro-inductive waveguide with electric interaction only between adjacent resonators. **a** Circuit with mutual capacitance. **b** Unit-cell transformed circuit model (see Appendix B.1) for a coplanar arrangement of resonators where wave propagation is backward

examples are power dividers [54], delay lines [58], passive chipless tags for radio-frequency identification (RFID) [60], and phase shifters [61].

2.4.2 Electro-Inductive Waves in Arrays of Electrically-Coupled Resonators

Electro-inductive waves (EIWs) can be regarded as the dual counterpart of magneto-inductive waves [62–65].⁴⁵ Therefore, EIWs propagate through a waveguide whose guiding mechanism is based on electric interaction between neighboring resonant elements, in parallelism (or duality) to MIWs. The lumped-element equivalent circuit model of a periodic electro-inductive waveguide with the first-neighbor approximation is depicted in Fig. 2.36a, where the mutual capacitance C_m accounts for the inter-resonator electric coupling. The resulting unit-cell equivalent-circuit model for a planar arrangement of electrically-coupled resonators, which supports backward propagation, is shown in Fig. 2.36b. As can be seen, for planar structures, the circuit of electro-inductive waveguides is dual to the circuit modeling magneto-inductive waveguides (Figs. 2.33c and 2.36b). This is not surprising because electromagnetic duality involves circuit duality, as was asserted in Sect. 2.3.5. Therefore, the dispersion relations inferred from the equivalent circuit models of magneto- and electro-inductive waveguides are equal to each other if the circuits are numerically dual. The meaningful difference lies in the nature (MIW- or EIW-related) of the propagating band.

⁴⁵However, propagation through electrically-coupled metallic rods have been known for a long time [66].

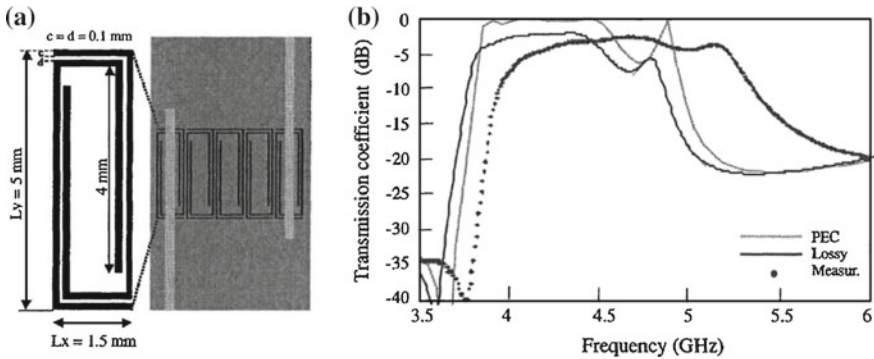


Fig. 2.37 Electro-inductive waves in an array of complementary split-ring resonators in coplanar configuration in microstrip implementation. **a** Layout and **b** simulated and measured transmission coefficient. Reprinted with permission from [62]

The first reported electro-inductive waveguide was implemented in microstrip technology using the complementary split squared ring resonator (CSSRR), that is, the complementary version of the SSRR [62]. Figure 2.37 shows the layout of the structure as well as the transmission coefficient. As expected, this waveguide behaves in a similar way as its dual counterpart⁴⁶ [58] (Fig. 2.35).

References

1. C. Caloz, T. Itoh, *Electromagnetic Metamaterials: Transmission Line Theory and Microwave Applications* (Wiley, New York, 2005)
2. N. Engheta, R.W. Ziolkowski, *Metamaterials: Physics and Engineering Explorations* (Wiley, New York, 2006)
3. R. Marqués, F. Martín, M. Sorolla, *Metamaterials with Negative Parameters: Theory, Design and Microwave Applications* (Wiley, New York, 2008)
4. G.V. Eleftheriades, K.G. Balmain, *Negative-Refractive Metamaterials: Fundamental Principles and Applications* (Wiley, New York, 2005)
5. L. Solymar, E. Shamonina, *Waves in Metamaterials* (Oxford University Press, New York, 2009)
6. F. Martín, *Artificial Transmission Lines for RF and Microwave Applications* (Wiley, New York, 2015)
7. S. Ramo, J.R. Whinnery, T. Van Duzer, *Fields and Waves in Communication Electronics* (Wiley, New York, 1965)
8. C.A. Balanis, *Advanced Engineering Electromagnetics* (Wiley, New York, 1989)
9. R.E. Collin, *Foundations for Microwave Engineering*, 2nd edn. (McGraw-Hill, New York, 1992)
10. D.M. Pozar, *Microwave Engineering*, 3rd edn. (Wiley, New York, 2005)
11. V.G. Veselago, The electrodynamics of substances with simultaneously negative values of ϵ and μ . *Physics-Uspekhi* **10**(4), 509–514 (1968)

⁴⁶In a strict sense, however, multilayer structures cannot be dual.

12. D.R. Smith, W.J. Padilla, D.C. Vier, S.C. Nemat-Nasser, S. Schultz, Composite medium with simultaneously negative permeability and permittivity. *Phys. Rev. Lett.* **84**(18), 4184–4187 (2000)
13. J.B. Pendry, A.J. Holden, D.J. Robbins, W.J. Stewart, Magnetism from conductors and enhanced nonlinear phenomena. *IEEE Trans. Microw. Theory Tech.* **47**(11), 2075–2084 (1999)
14. A.K. Iyer, G.V. Eleftheriades, Negative refractive index metamaterials supporting 2-D waves, in *IEEE MTT-S International Microwave Symposium Digest*, vol. 2 (Seattle, WA, USA, 2002). pp. 1067–1070
15. A.A. Oliner, A periodic-structure negative-refractive-index medium without resonant elements, in *IEEE-AP-S USNC/URSI National Radio Science Meeting* (San Antonio, TX, USA, 2002). p. 41
16. C. Caloz, T. Itoh, Application of the transmission line theory of left-handed (LH) materials to the realization of a microstrip “LH line”, in *IEEE-AP-S USNC/URSI National Radio Science Meeting*, vol. 2 (2002). pp. 412–415
17. C. Caloz, T. Itoh, Novel microwave devices and structures based on the transmission line approach of meta-materials, in *IEEE MTT-S International Microwave Symposium Digest*, vol. 1 (Philadelphia, PA, USA, 2003). pp. 195–198
18. J.S. Hong, M.J. Lancaster, *Microstrip Filters for RF/Microwave Applications* (Wiley, New York, 2001)
19. A. Grbic, G.V. Eleftheriades, Experimental verification of backward-wave radiation from a negative refractive index metamaterial. *J. Appl. Phys.* **92**(10), 5930–5935 (2002)
20. F. Martín, J. Bonache, F. Falcone, M. Sorolla, R. Marqués, Split ring resonator-based left-handed coplanar waveguide. *Appl. Phys. Lett.* **83**(22), 4652–4654 (2003)
21. J.D. Baena, J. Bonache, F. Martín, R.M. Sillero, F. Falcone, T. Lopetegi, M.A.G. Laso, J. García-García, I. Gil, M.F. Portillo, M. Sorolla, Equivalent-circuit models for split-ring resonators and complementary split-ring resonators coupled to planar transmission lines. *IEEE Trans. Microw. Theory Tech.* **53**(4), 1451–1461 (2005)
22. F. Falcone, T. Lopetegi, J.D. Baena, R. Marqués, F. Martín, M. Sorolla, Effective negative- ϵ ; stopband microstrip lines based on complementary split ring resonators. *IEEE Microw. Wirel. Compon. Lett.* **14**(6), 280–282 (2004)
23. F. Falcone, T. Lopetegi, M. Laso, J. Baena, J. Bonache, M. Beruete, R. Marqués, F. Martín, M. Sorolla, Babinet principle applied to the design of metasurfaces and metamaterials. *Phys. Rev. Lett.* **93**(197401) (2004)
24. F. Aznar, J. Bonache, F. Martín, Improved circuit model for left-handed lines loaded with split ring resonators. *Appl. Phys. Lett.* **92**(043512) (2008)
25. J. Bonache, M. Gil, O. García-Abad, F. Martín, Parametric analysis of microstrip lines loaded with complementary split ring resonators. *Microw. Opt. Technol. Lett.* **50**(8), 2093–2096 (2008)
26. F. Martín, F. Falcone, J. Bonache, R. Marqués, M. Sorolla, Miniaturized coplanar waveguide stop band filters based on multiple tuned split ring resonators. *IEEE Microw. Wirel. Compon. Lett.* **13**(12), 511–513 (2003)
27. I.J. Bahl, P. Bhartia, *Microwave Solid State Circuit Design* (Wiley, New York, 2003)
28. F. Aznar, M. Gil, J. Bonache, L. Jelinek, J.D. Baena, R. Marqués, F. Martín, Characterization of miniaturized metamaterial resonators coupled to planar transmission lines through parameter extraction. *J. Appl. Phys.* **104**(114501) (2008)
29. J. Bonache, M. Gil, I. Gil, J. García-García, F. Martín, On the electrical characteristics of complementary metamaterial resonators. *IEEE Microw. Wirel. Compon. Lett.* **16**(10), 543–545 (2006)
30. L. Brillouin, *Wave Propagation in Periodic Structures: Electric Filters and Crystal Lattices* (McGraw-Hill, New York, 1946)
31. F. Aznar, M. Gil, J. Bonache, F. Martín, Modelling metamaterial transmission lines: a review and recent developments. *Opto Electron. Rev.* **16**(3), 226–236 (2008)
32. F. Bilotti, L. Vegni, From metamaterial-based to metamaterial-inspired miniaturized antennas: A possible procedure and some examples, in *Proceedings of URSI XXIX General Assembly* (2008) pp. 1–4

33. K. Chang, L.-H. Hsieh, *Microwave Ring Circuits and Related Structures* (Wiley, New York, 2004)
34. J. Martel, R. Marqués, F. Falcone, J. Baena, F. Medina, F. Martín, M. Sorolla, A new LC series element for compact bandpass filter design. *IEEE Microw. Wirel. Compon. Lett.* **14**(5), 210–212 (2004)
35. A. Vélez, F. Aznar, J. Bonache, M. Velázquez-Ahumada, J. Martel, F. Martín, Open complementary split ring resonators (OCSRRs) and their application to wideband CPW band pass filters. *IEEE Microw. Wirel. Compon. Lett.* **19**(4), 197–199 (2009)
36. W.N. Hardy, L.A. Whitehead, Split-ring resonator for use in magnetic resonance from 200–2000 MHz. *Rev. Sci. Instrum.* **52**(2), 213–216 (1981)
37. C.A. Balanis, *Antenna Theory: Analysis and Design*, 2nd edn. (Wiley, New York, 1997)
38. R. Marqués, F. Medina, R. Rafii-El-Idrissi, Role of bianisotropy in negative permeability and left-handed metamaterials. *Phys. Rev. B* **65**(144440) (2002)
39. P. Gay-Balmaz, O.J.F. Martín, Electromagnetic resonances in individual and coupled split-ring resonators. *J. Appl. Phys.* **92**(5), 2929–2936 (2002)
40. N. Katsarakis, T. Koschny, M. Kafesaki, E. Economou, C. Soukoulis, Electric coupling to the magnetic resonance of split ring resonators. *Appl. Phys. Lett.* **84**(15), 2943–2945 (2004)
41. M. Shamonin, E. Shamonina, V. Kalinin, L. Solymar, Properties of a metamaterial element: analytical solutions and numerical simulations for a singly split double ring. *J. Appl. Phys.* **95**(7), 3778–3784 (2004)
42. M. Shamonin, E. Shamonina, V. Kalinin, L. Solymar, Resonant frequencies of a split-ring resonator: analytical solutions and numerical simulations. *Microw. Opt. Technol. Lett.* **44**(2), 133–136 (2005)
43. J. García-García, F. Martín, J.D. Baena, R. Marqués, L. Jelinek On the resonances and polarizabilities of split ring resonators. *J. Appl. Phys.* **98**(033103) (2005)
44. R. Marqués, J. Baena, J. Martel, F. Medina, F. Falcone, M. Sorolla, F. Martín, Novel small resonant electromagnetic particles for metamaterial and filter design, in *International Conference on Electromagnetics in Advanced Applications (ICEAA '03)* (Torino, Italy, 2003). pp. 439–442
45. M. Makimoto, S. Yamashita, Compact bandpass filters using stepped impedance resonators. *Proc. IEEE* **67**(1), 16–19 (1979)
46. D. Schurig, J. Mock, D. Smith, Electric-field-coupled resonators for negative permittivity metamaterials. *Appl. Phys. Lett.* **88**(041109) (2006)
47. H. Booker, Slot aerials and their relation to complementary wire aerials (Babinet's principle). *J. IEE Part IIIA* **93**(4), 620–626 (1946)
48. R. King, G.H. Owyang, Complementarity in the study of transmission lines. *IEEE Trans. Microw. Theory Tech.* **8**(2), 172–181 (1960)
49. C.-S. Kim, J.-S. Park, D. Ahn, J.-B. Lim, A novel 1-D periodic defected ground structure for planar circuits. *IEEE Microw. Guided Wave Lett.* **10**(4), 131–133 (2000)
50. T. Hand, J. Gollub, S. Sajuyigbe, D. Smith, S. Cummer, Characterization of complementary electric field coupled resonant surfaces. *Appl. Phys. Lett.* **93**(212504) (2008)
51. W. Getsinger, Circuit duals on planar transmission media, in *IEEE MTT-S International Microwave Symposium Digest* (Boston, MA, USA, 1983). pp. 154–156
52. J. Naqui, M. Durán-Sindreu, F. Martín, Differential and single-ended microstrip lines loaded with slotted magnetic-LC (MLC) resonators. *Int. J. Antennas Propag.* **2013**(640514) (2013)
53. E. Shamonina, V.A. Kalinin, K.H. Ringhofer, L. Solymar, Magneto-inductive waveguide. *Electron. Lett.* **38**(8), 371–373 (2002)
54. E. Shamonina, V.A. Kalinin, K.H. Ringhofer, L. Solymar, Magnetoinductive waves in one, two, and three dimensions. *J. Appl. Phys.* **92**(10), 6252–6261 (2002)
55. V. Lomanets, O. Zhurumskyy, G. Onishchukov, O. Sydoruk, E. Tatartschuk, E. Shamonina, G. Leuchs, U. Peschel, Interacting waves on chains of split-ring resonators in the presence of retardation. *Appl. Phys. Lett.* **97**(011108) (2010)
56. I.V. Shadrivov, A.N. Reznik, Y.S. Kivshar, Magnetoinductive waves in arrays of split-ring resonators. *Physica B Condens. Matter* **394**(2), 180–183 (2007)

57. R.R.A. Syms, E. Shamonina, L. Solymar, Positive and negative refraction of magnetoinductive waves in two dimensions. *Europ. Phys. J. B* **46**(2), 301–308 (2005)
58. M.J. Freire, R. Marqués, F. Medina, M.A.G. Laso, F. Martín, Planar magnetoinductive wave transducers: theory and applications. *Appl. Phys. Lett.* **85**(19), 4439–4441 (2004)
59. R.R.A. Syms, E. Shamonina, L. Solymar, Magneto-inductive waveguide devices. *IEE Proc. Microw. Antennas Propag.* **153**(2), 111–121 (2006)
60. F.J. Herraiz-Martínez, F. Paredes, G. Zamora González, F. Martín, J. Bonache, Printed magnetoinductive-wave (MIW) delay lines for chipless RFID applications. *IEEE Trans. Antennas Propag.* **60**(11), 5075–5082 (2012)
61. I.S. Nefedov, S.A. Tretyakov, On potential applications of metamaterials for the design of broadband phase shifters. *Microw. Opt. Technol. Lett.* **45**(2), 98–102 (2005)
62. M. Beruete, F. Falcone, M.J. Freire, R. Marqués, J.D. Baena, Electroinductive waves in chains of complementary metamaterial elements. *Appl. Phys. Lett.* **88**(083503) (2006)
63. R.R.A. Syms, L. Solymar, A generic approach to boundary reflection in periodic media. *Eur. Phys. J. B* **54**(2), 169–174 (2006)
64. M. Aznabet, O. El Mrabet, M. Navarro, M. Beruete, F. Falcone, M. Essaaidi, M. Sorolla, Wave propagation properties in stacked SRR/CSRR metasurfaces at microwave frequencies, in *Mediterranean Microwave Symposium (MMS)* (Tangier, Morocco, 2009)
65. M. Beruete, M. Aznabet, M. Navarro-Cía, O. El Mrabet, F. Falcone, N. Akin, M. Essaaidi, M. Sorolla, Electroinductive waves role in left-handed stacked complementary split rings resonators. *Opt. Exp.* **17**(3), 1274–1281 (2009)
66. J. Shefer, Periodic cylinder arrays as transmission lines. *IEEE Trans. Microw. Theory Tech.* **11**(1), 55–61 (1963)

Symmetry Properties in Transmission Lines Loaded with
Electrically Small Resonators
Circuit Modeling and Applications

Naqui, J.

2016, XX, 210 p., Hardcover

ISBN: 978-3-319-24564-5